

## 1 ENQUIRE RECONSTRUCTS AND EXPANDS CONTEXT-SPECIFIC CO- 2 OCCURRENCE NETWORKS FROM BIOMEDICAL LITERATURE

3 Luca Musella<sup>1\*</sup>, Xin Lai<sup>1, 2</sup>, Max Widmann<sup>1</sup> and Julio Vera<sup>1\*</sup>

4 <sup>1</sup>Laboratory of Systems Tumor Immunology, Friedrich-Alexander-Universität Erlangen-Nürnberg,  
5 Deutsches Zentrum Immuntherapie, BZKF, and Uniklinikum Erlangen, Erlangen, Germany

6 <sup>2</sup>Systems and Network Medicine Lab, Biomedicine Unit, Faculty of Medicine and Health Technology,  
7 Tampere University, Tampere, Finland

8 \*To whom correspondence should be addressed. Tel: +49 9131 85-45899; Email: luca.musella@uk-  
9 erlangen.de

10 Correspondence may also be addressed to Julio Vera. Tel: Tel: +49 9131 85-45876; Email: julio.vera-  
11 gonzalez@uk-erlangen.de

### 12 ABSTRACT

13 The accelerating growth of scientific literature overwhelms our capacity to manually distil  
14 complex phenomena like molecular networks linked to diseases. Moreover, biases in biomedical  
15 research and database annotation limit our interpretation of facts and generation of hypotheses.  
16 ENQUIRE (Expanding Networks by Querying Unexpectedly Inter-Related Entities) offers a  
17 time- and resource-efficient alternative to manual literature curation and database mining.  
18 ENQUIRE reconstructs and expands co-occurrence networks of genes and biomedical ontologies  
19 from user-selected input corpora and network-inferred PubMed queries. The integration of text  
20 mining, automatic querying, and network-based statistics mitigating literature biases makes  
21 ENQUIRE unique in its broad-scope applications. For example, ENQUIRE can generate co-  
22 occurrence gene networks that reflect high-confidence, functional networks. When tested on case  
23 studies spanning cancer, cell differentiation and immunity, ENQUIRE identified interlinked  
24 genes and enriched pathways unique to each topic, thereby preserving their underlying diversity.  
25 ENQUIRE supports biomedical researchers by easing literature annotation, boosting hypothesis  
26 formulation, and facilitating the identification of molecular targets for subsequent  
27 experimentation.

28

29

## GRAPHICAL ABSTRACT

Scientific Problem	Systems biologists need networks to better interpret omics data	Clinicians need context-aware pathways to assign drug therapies	Modellers and experimentalists need annotated gene sets to construct biological models
	“Ferroptosis AND Immune System”, “Ferroptosis AND Mitochondria”	“ANGPT1 mutations” (Case A), “SLC9A1 mutations” (Case B)	“Ferroptosis AND Neovascularization”
Workflow			
Query-Specific Networks	Source Query ● “Ferroptosis” AND “Immune System” ● “Ferroptosis” AND “Mitochondria” ● Both ● Node Degree	Context-Aware Pathway Enrichment	Automatic Gene Set Annotation

30

31

## 32 INTRODUCTION

33 Curated gene networks are of high interest to prime the analysis of biomedical omics data, identification of disease-specific regulatory modules, and therapy-oriented studies like drug repurposing<sup>1–4</sup>. However, the growing biomedical literature corpus makes curation of biomolecular pathways challenging. Annotating molecular interactions from literature requires domain expertise, yet that same background knowledge could entail predispositions towards partial pictures of faceted biomedical problems<sup>5</sup>. In contrast, relation extraction from databases often omits the contextual information of gene interactions and can bias the results towards ubiquitously expressed, commonly investigated, and richly annotated genes<sup>6–8</sup>. This can make systematic comparisons of biomedical research topics inconclusive or unattractive from an expenditure perspective. Recently, there have been significant investments in the automatic annotation of scientific corpora. The knowledgebase immuneXpresso indexes textmined interactions among immune cells and cytokines<sup>9</sup>, while SimText provides a framework to interactively explore the content of a user-provided corpus of literature<sup>10</sup>. These and other tools rely on natural language processing methods like named-entity recognition<sup>11</sup> (NER), part-of-speech recognition<sup>12</sup>, directionality assignment<sup>13</sup>, relationship detection, and co-occurrence scoring<sup>14,15</sup>. These efforts in biomedical text mining aim at detecting meta-features and co-occurrences in literature corpora. However, assessing the statistical significance and confidence level of a text-mined relation in dense, literature-based co-occurrence networks must be better addressed<sup>16,17</sup>. We find this striking, considering the well-documented reproducibility crisis<sup>18–20</sup>. In this context, we envisioned ENQUIRE (Expanding Networks by Querying Unexpectedly Inter-Related Entities) to achieve automatic reconstruction and expansion of biomedical co-occurrence networks from a user-defined PubMed literature corpus. ENQUIRE applies a state-of-the-art random graph model to retrieve context-specific, significant co-occurrences, i.e. dependent on the input corpus and its occurrence distribution of biomedical entities<sup>21,22</sup>. This distinctive element in our methodology allows ENQUIRE to control for literature biases. ENQUIRE processes scientific articles by extracting Medical Subject Headings (MeSH) and gene mentions from article abstracts, thus enriching gene-gene co-occurrence networks with gene-MeSH and MeSH-MeSH relations. ENQUIRE also automatically generates PubMed queries from connected biomedical entities in the network, contextually expanding the underlying corpus and, in turn, the co-occurrence network. To our knowledge, ENQUIRE is the first tool that integrates textmining, network reconstruction, and automatic literature querying into a single, resource efficient software. Here, we showcase ENQUIRE’s broad-scope applications and effectiveness in identifying relevant biomedical relations in different contexts and case scenarios.

## 64 RESULTS

### 65 A Tool to Generate Co-Occurrence Networks from Literature

66 ENQUIRE (Expanding Networks by Querying Unexpectedly Inter-Related Entities) is an algorithm that reconstructs and expands co-occurrence networks of *Homo sapiens* genes and biomedical ontologies (MeSH), using a corpus of PubMed articles as input. The method iteratively annotates MeSH and gene mentions from abstracts, statistically assesses their importance, and generates network-informed PubMed queries, until it obtains a connected network of genes and MeSH terms (or meets another exit condition). ENQUIRE’s pipeline implements a loop consisting of serial modules with the following structure (**Fig. 1**):

73 a) The user supplies an input literature corpus in the form of at least three PubMed identifiers (PMIDs).  
74 b) The algorithm indexes the MeSH terms associated to the PMIDs listed. Next, their abstracts are  
75 parsed, and gene normalization is performed using a lookup table of gene aliases and abstract-specific  
76 blocklists of ambiguous terms.

77 c) ENQUIRE annotates and weights co-occurrences between gene and MeSH entities, accounting for  
78 the expected number of co-occurrences across the literature corpus.

79 d) The method selects significant co-occurrences and generates an undirected, simple graph, basing  
80 the test statistic on a random graph null model of unbiased mining of the input corpus.

81 e) Next, nodes are weighted, and “information-dense” maximal cliques, i.e. clusters of high-weight  
82 nodes all connected to each other, are selected to reconstruct network communities from the  
83 corresponding nodes.

84 f) ENQUIRE identifies optimal sets of community-connecting graphlets via an approximate solution  
85 to the “travelling salesman problem” (TSP).

86 g) Finally, the algorithm uses the entity nodes corresponding to the identified community-connecting  
87 graphlets into PubMed queries to find additional, relevant articles. Should ENQUIRE find new articles,  
88 their PMIDs are joined with the previous ones and automatically provided to module a), starting a new  
89 iteration.

90 Whenever ENQUIRE reconstructs a network from the union of old and new PMIDs, the previously  
91 reconstructed network is joined with the new one. The joined network has recomputed edge and node  
92 weights in accordance to its expanded literature corpus and connectivity. The rationale is to prioritize  
93 the original reconstruction, while also leveraging the expanded literature corpus. Users can tune five  
94 options to tailor the workflow, namely: 1) Restricting the target entities to annotate genes or MeSH  
95 only – default: both; 2) representativeness threshold  $t$  to disregard subgraphs characterized by poor  
96 overlap with the literature corpus – default: 1% overlap; 3) query size  $k$  to control the number of  
97 entities that must be simultaneously used in a PubMed query – default: 4 entities; 4) query attempts  $A$   
98 to choose the number of attempts at connecting network communities by querying – default: 2  
99 attempts; and 5) connectivity criterion  $K$  to exclude newly found entities not having edges with nodes  
100 from  $K$  communities previously generated at step (e) – default: 2 communities. ENQUIRE’s goal is to  
101 generate a gene/MeSH network and its respective gene- and MeSH-only subgraphs that individually  
102 consist of a single, connected component. The loop terminates if i) the network is empty after module  
103 d); ii) no clique can be found in step e); iii) the clique network consists of only one community; iv) all  
104 generated queries return empty results. With default parameters, ENQUIRE outputs node and edge  
105 lists of a gene/MeSH co-occurrence network and the respective gene- and MeSH-only subgraphs at  
106 each iteration. The final ENQUIRE results include additional tabulated data, graphics, and links to  
107 collected resources for subsequent analyses and reproducibility. For instance, it is possible to extract  
108 subsets of the literature corpus that support a gene/MeSH relation of interest and access the articles via  
109 hyperlinks redirecting to PubMed.

110 See **Supp. Fig. 1** and **Mat.Met.** for a comprehensive description of the algorithm.

## 111 **An Exemplary ENQUIRE Run**

112 To showcase ENQUIRE, we set up a small-scale case study in which we looked for literature-based  
113 relationships between the immune system and ferroptosis, a form of programmed cell death<sup>23</sup>. We  
114 selected 27 papers obtained from the PubMed query (“*Ferroptosis*”[MeSH terms] AND “*Immune*  
115 *System*”[MeSH terms]) NOT “*review*”[Publication Type] – queried on 14.04.23. We increased the  
116 number of attempts  $A$  to 3, as we expected few query-matching PMID. The expansion process is  
117 depicted in **Fig. 2A**, using the Cytoscape package DyNet<sup>24,25</sup>. The original reconstructed network  
118 consists of four connected components. The first expansion led to additional, significant co-  
119 occurrences and newly found entities that connected the four components into a single one. The  
120 algorithm stopped after obtaining a single, connected gene/MeSH network and not finding additional  
121 query-matching PMIDs. Using up to 6 CPU cores, ENQUIRE finished in 16 minutes using less than  
122 0.4 GB of RAM (**Supp. Fig. 2**). Next, we applied context-specific gene set annotation on the original  
123 gene/MeSH co-occurrence networks, as described in **Mat.Met.** We identified non-trivial, descriptive

124 gene sets (**Fig. 2C-left**), including ferroptosis-dependent inflammation supported by immune-related  
125 adaptor proteins (blue, top left), antineoplastic effects of the ferroptosis-inducer sulfasalazine acting  
126 on the amino acid transport system (magenta), and cross-talk between ferroptosis and autophagy  
127 (pink), in accordance with previous findings<sup>26-28</sup>. We also performed context-aware pathway  
128 enrichment analysis using the gene-gene co-occurrence subgraphs and the approach described in  
129 **Mat.Met**. We summarized the results in **Fig. 2C-right**, which depicts 30 Reactome pathways whose  
130 adjusted p-values were below 5% FDR for at least one network, sorted by Reactome category. In the  
131 original network, we obtained enrichments of pathways centered around Toll-like receptor and MAP  
132 kinases signaling cascades (e.g. R-HSA-975138). In the expanded networks, the metabolic pathway  
133 *Glutathione conjugation* (R-HSA-156590) and additional innate immunity-related and programmed  
134 cell death pathways were enriched. Taken together, the ENQUIRE-generated output highlights  
135 potential molecular axes between iron-regulated cell death and proliferation, metabolism, and immune  
136 response<sup>29-31</sup>.

### 137 **ENQUIRE's Gene Normalization Strategy is Precise and Efficient**

138 ENQUIRE is intended to consume abstracts from studies in *H. sapiens* and *M. musculus*. We therefore  
139 evaluated ENQUIRE's precision and recall using the abstracts in the NLM-Gene corpus mentioning at  
140 least one *M. musculus* or *H. sapiens* gene – 479 out of 550 entries<sup>32</sup>. ENQUIRE's maximum F1 score  
141 is 0.747, corresponding to 0.822 precision and 0.683 recall, using as little as 0.36 GB of RAM and  
142 with speeds up to 0.03 seconds per abstract (**Table 1**). The Schwartz-Hearst abbreviation-definition  
143 detection algorithm improves precision of tokenization and normalization by 2%, without major loss  
144 in recall nor higher computational requirements<sup>33</sup>. In some use cases, it could be necessary to exclude  
145 gene mentions associated to cell entities, such as “CD8+ lymphocytes”. The scispaCy's  
146 *en\_ner\_jnlpba\_md* model removes unwanted gene-matching cell mentions, at the cost of about 2%  
147 reduction in recall<sup>34</sup>. It should be noted, however, that the latter metric is affected by the fact that gene  
148 mentions included in cell entities are counted as true positives in the NLM-Gene corpus. We also  
149 compared ENQUIRE's performance to GNorm2, a state-of-the-art deep-learning model for gene entity  
150 recognition and normalization<sup>35</sup>. We tested ENQUIRE's most resource-intensive configuration (both  
151 *en\_ner\_jnlpba\_md* and *Schwartz-Hearst* modules enabled) against GNorm2's implementation of  
152 Bioformer, a deep-learning model based on BERT, but 60% smaller in size<sup>36</sup>. **Table 2** shows that  
153 GNorm2 is considerably slower and has a higher resource usage than ENQUIRE. If ENQUIRE were  
154 to implement GNorm2 for gene normalization, this would impair its usage in scenarios with limited  
155 resources and computing time: for example, we verified that GNorm2 cannot be run on the CPU-based  
156 computer with 16GB of RAM used for the exemplary case study (**Supp. Fig. 3** and **Supp.**  
157 **Information**). In this terms, ENQUIRE's *in-house* gene normalization is more suitable for textmining  
158 large input corpora on a variety of devices beyond CPU-based computer clusters.

### 159 **ENQUIRE Networks Support Ranking of Genes Relevant to the Input Literature.**

160 To evaluate ENQUIRE's ability in inferring genes relevant to the input corpus, we extracted *H. sapiens*  
161 pathways, their belonging genes, and corresponding primary literature references from the Reactome  
162 Graph Database<sup>37</sup>. We used the lists of references as inputs and performed a single gene entity-  
163 restricted co-occurrence network reconstruction for each pathway. Out of 967 examined pathways,  
164 ENQUIRE successfully reconstructed a gene co-occurrence network from the reference literature of  
165 733 of them. We evaluated the effect of input corpus size, pathway size and average entity co-  
166 occurrence per paper on the accuracy of the resulting networks (**Table 3**). As expected, precision and  
167 recall show opposite Spearman's correlation trends concerning corpus and pathway sizes, but average  
168 gene-gene co-occurrence per article appears uncorrelated. The negative correlation between corpus  
169 size and precision is -0.18, suggesting a low impact of large input corpora on the output. Next, we

170 explored if the ENQUIRE-computed weight  $W$ , an aggregated measure of network centrality and  
171 literature support of its connections, is a useful measure of gene relevance regarding the input corpus  
172 (**Mat.Met.**). To this end, we analyzed the above-mentioned gene-scope co-occurrence networks. In  
173 **Fig. 3**, we compare the pan-pathway-aggregated distributions of true-positive (top panel) and false-  
174 positive (middle panel) ENQUIRE-derived genes as a function of  $W$  (x-axis). We subdivided the  
175 distribution into four evenly spaced intervals, performed a chi-square test of independence, which  
176 resulted to be significant, and extracted the standardized Pearson residuals for true positives and false  
177 positives (colored boxes beneath the distributions). True positives tend to have higher node weights  
178 than false positives. An over-representation of node weights higher than 0.75 is observed in the true-  
179 positive distribution, as indicated by the color gradient in Pearson residuals. This suggests one can use  
180 the node weights  $W$  to rank a set of ENQUIRE-derived genes based on their relevance to the literature  
181 corpus in question.

## 182 **ENQUIRE Recovers Genes with High Chances of Showing Biochemical Interrelations.**

183 We hypothesized that ENQUIRE-derived gene co-occurrence networks could be enriched in molecular  
184 gene-gene interactions annotated in databases. To test this, we queried PubMed with all possible cross-  
185 pairs of *Diseases* and *Genetic Phenomena* MeSH terms. We further processed the 3098 queries that  
186 retrieved 50-500 matching PMIDs and extracted their gene-gene co-occurrence networks obtained  
187 after one network reconstruction. We then inspected whether their respective protein-coding genes can  
188 produce significant functional association networks based on STRING's protein-protein interaction  
189 (PPI) database<sup>38</sup> (see **Mat.Met.**). **Table 4** indicates that for 1336 (43.1%) MeSH pairs, both ENQUIRE  
190 and STRING generated a minimal network with at least three genes and two edges. In a subset of 733  
191 network with degree sequences allowing at least ten different graph realizations, we assessed  
192 ENQUIRE's capability of reflecting functional interactions. Then, we then generated two empirical  
193 random probability distributions for STRING's edge count and DeltaCon similarity score<sup>39</sup> (see  
194 **Mat.Met.**). Within the tested networks, 730 protein-coding gene networks (99.6%) produced a  
195 STRING network with a higher edge count than 95% of equal-sized random STRING networks (PPI  
196 score). At the same time, 439 networks (59.9%) showed concordance with STRING-derived PPI  
197 networks based on statistically significant DeltaCon similarities. After p-value adjustment, (1% FDR,  
198 **Table 3**), 722 (98.5%) and 344 (46.9%) ENQUIRE networks still show significantly high PPI scores  
199 and DeltaCon similarities, respectively. To evaluate the effect of network size, we subdivided the 733  
200 suitable networks into quartiles based on their node number and mapped the respective unadjusted p-  
201 value distributions of the above-described test sets. The edge-count-associated p-values increased with  
202 network size (**Fig. 4A**). At the same time, the observed DeltaCon similarity values monotonically  
203 decrease with network size (**Table 5**). This is in accordance with DeltaCon's implementation of edge  
204 importance and zero-property<sup>39</sup>, as differences in edge counts and number of connected components  
205 between ENQUIRE and STRING increase with the number of nodes. Nevertheless, we did not find a  
206 negative correlation between network size and p-values of observed DeltaCon similarities; instead, the  
207 quartile corresponding to the largest network also shows the largest relative proportion of significant  
208 adjusted p-values (**Fig. 4B**). Taken together, our results suggest that ENQUIRE generates networks  
209 that frequently contain established, high-confidence functional relations.

## 210 **ENQUIRE Improves the Context Resolution of Topology-Based Pathway Enrichment 211 Analyses.**

212 We also analyzed ENQUIRE's ability to generate and expand co-occurrence networks with distinctive  
213 biological and biomedical signatures by literature querying. In particular, we evaluated the context  
214 resolution of ENQUIRE-generated gene networks, i.e. their ability to preserve differences and  
215 similarities in gene mention content from different corpora. To this end, we applied the complete

216 ENQUIRE pipeline with default parameters to a comprehensive set of case studies, spanning cancer,  
217 cell differentiation, innate immunity, autoimmune diseases, and a positive control (**Table 6**). Notice  
218 that each case study's input corpus is a perfect subset of the positive control corpus, which corresponds  
219 to a Szymkiewicz-Simpson overlap coefficient (OC) of 100% - see **Mat.Met.**. Despite that, the positive  
220 control network does not always exhibit an OC of 100% with non-expanded networks, in terms of both  
221 nodes and edges (**Supp. Fig. 4**). This shows that ENQUIRE's network reconstruction is sensitive to  
222 the input corpus. **Fig. 5A** depicts the expected dendrogram of the different case studies and respective  
223 expansions, based on their major topics and original input corpora. **Fig. 5B** shows the observed  
224 clustering based on ENQUIRE-informed, topology-based pathway enrichment analysis using KNet<sup>40</sup>  
225 (see Post Hoc Analyses in **Mat.Met.** and **Supp. Fig. 2**). The 50 pathways with at least one significant,  
226 adjusted p-value (5% FDR) and highest p-value variances across case studies are depicted. The heat-  
227 map suggests that the case studies primarily cluster based on the affinities between their major topics,  
228 in agreement with the expected dendrogram. For example, pathways categorized under *Diseases of*  
229 *Metabolism*, *Diseases of Immune System*, and *Innate Immune System* are predominantly enriched in  
230 networks originated from the case study "Macrophage's signal transduction during M. tuberculosis  
231 infection" (MP-ST) and the major topic "Antigen Presentation in Autoimmune Diseases". Similarly,  
232 some of *Chromatin Organization* and *Developmental Biology* pathways are almost exclusively  
233 enriched in the networks corresponding to oligodendrocyte differentiation. Interestingly, a set of  
234 pathways linked to cell cycle like *Cyclin D associated events in G1* (R-HSA-69231) are enriched in  
235 the oligodendrocyte case study and reported to be also relevant in glioblastoma<sup>41-44</sup>. All case studies  
236 appear constitutively enriched in a cluster of *Pathways in Cancer* annotated downstream of *Diseases*  
237 of *signal transduction by growth factor receptors and second messengers* (R-HSA-5663202). We  
238 investigated this potential limitation in context-resolution and found that i) KNet-employed, binned  
239 network distances between genes in R-HSA-5663202 subpathways are not significantly smaller than  
240 those within other tested pathways; ii) Spearman correlations between p-values and network or corpus  
241 sizes are equivalent in all tested pathways; iii) R-HSA-5663202 subpathway categorization is  
242 associated with lower p-values both globally and within the same major topic (**Supp. Fig. 5**). Perhaps  
243 unsurprisingly, we concluded that proteins from these pathways like MAP-kinases and PKB are  
244 generally involved in the explored case studies; this also suggests that the observed clustering of  
245 cancer-related studies is not exclusively dependent on the enrichment of cancer pathways. Finally, we  
246 quantitatively assess the context resolution of the ENQUIRE-informed enrichment (**Fig. 5C**). To this  
247 end, we performed a permutation test on the observed Baker's gamma correlation value between  
248 dendrograms (**Fig. 5A-B**), which allows to statistically assess their similarity<sup>45</sup>. We benchmarked its  
249 significance against two other methods, namely gene set over-representation analysis (ORA), and  
250 topology-based pathway enrichment analysis using STRING's high-confidence functional  
251 associations, instead of ENQUIRE-generated co-occurrences, to compute the *Q* node scores (see  
252 **Mat.Met.**). All methods generated a dendrogram significantly closer than expected to the reference.  
253 In our analysis, topology-based enrichments outperform ORA, with the ENQUIRE-informed score  
254 moderately improving the performance over the STRING-informed equivalent (0.69 and 0.64,  
255 respectively). Taken together, these results suggest that ENQUIRE-generated networks can effectively  
256 represent contextual, biological differences and similarities between case study corpora. While  
257 ENQUIRE-annotated genes are sufficient for context resolution, the use of topology-based methods  
258 that incorporate corpus-specific co-occurrence information improves the performance.  
259

260 **DISCUSSION**

261 ENQUIRE is a novel computational framework that combines textmining, network reconstruction, and  
262 literature querying, offering an alternative to manual literature curation and database mining.  
263 ENQUIRE interrelates gene mentions and biomedical concepts through co-occurrence networks and  
264 tabulated references while accounting for biases in the input literature corpus. Its framework enables  
265 *post hoc* analyses that infer contextual gene sets and enriched molecular pathways. ENQUIRE can  
266 enhance the biological interpretation of omics data, suggest relevant processes and components for  
267 computational models, and motivate the selection of molecular targets for biological experiments and  
268 in scenarios like molecular tumor boards. We opted for a compromise between coverage of  
269 unannotated article abstracts (gene normalization) and high-fidelity, pre-computed concept annotations  
270 (MeSH retrieval). ENQUIRE's gene normalization strategy is appropriate for reconstructing co-  
271 occurrence gene networks with affordable computational requirements, and scales well with large input  
272 corpora, without the need of restricting the analysis to databases of pre-annotated gene mentions<sup>46</sup>. The  
273 combination of a curated lookup table with abstract-specific blocklists enhances precision, thus leading  
274 to co-occurrence networks with fewer false positives, compared to recall-oriented approaches like  
275 BERN2<sup>35,47</sup>. An added value of ENQUIRE is that the obtained gene/MeSH co-occurrence network can  
276 prime further information retrieval beyond textmining. Differently from previous works on  
277 gene/MeSH relations, our statistical framework is independent of the user scope (genes or MeSH can  
278 be mined separately) and is not immutable with respect to a species or general topic (e.g. diseases)<sup>48–</sup>  
279 <sup>51</sup>. Instead, ENQUIRE automatically constructs PubMed queries from network-derived genes and  
280 MeSH to expand the input corpus, and in turn the network. We also assessed ENQUIRE's performance  
281 using real-world case scenarios. For example, we investigated the relationship between ENQUIRE-  
282 suggested co-occurrences and database-annotated gene interactions. Our results indicate that  
283 ENQUIRE-generated gene co-occurrence networks reflect experimental and database-annotated  
284 functional gene associations. At the same time, ENQUIRE can also generate networks with previously  
285 unannotated wirings that can encourage novel explorative analyses (**Fig. 4B**). We also analyzed the  
286 feasibility of corroborating ENQUIRE-suggested relations by mapping co-occurrence information  
287 onto a mechanistic reference network. Since there is no generalizable method to project a network of  
288 indirect relations (co-occurrences) onto a mechanistic network<sup>52–56</sup>, we designed a function to score a  
289 physical interaction network using ENQUIRE-generated networks. This allowed us to verify that the  
290 enriched pathways in original and expanded ENQUIRE networks reflect their contexts and enable the  
291 comparison of multiple case studies. This strategy still poses some limitations in terms of choosing a  
292 reference network and pathways to be tested. We designed ENQUIRE as a series of modular, open-  
293 source components that can be combined and expanded to tune its performance. For instance, one  
294 could insert a part-of-speech recognition parser upstream of the co-occurrence detection step to  
295 strengthen its criteria<sup>57</sup>. Similarly, one can implement a propensity matrix into the random graph model  
296 to further weight a co-occurrence with its textual context<sup>14,21</sup>. As gene normalization relies on the  
297 utilized lookup table of reference gene symbols and aliases, ENQUIRE's accuracy depends on how  
298 comprehensive and free of ambiguities this table is. The current version of our algorithm only performs  
299 normalization of human genes and corresponding mouse orthologs. Still, it can be adapted to perform  
300 gene normalization of any other species by supplying an appropriate lookup table, such as those  
301 provided by the STRING database<sup>58</sup>. Our main objective was to construct a robust textmining, network  
302 reconstruction, and automatic querying pipeline accessible to bioinformaticians and systems biologists  
303 with affordable computational requirements. Since the standalone version of the algorithm requires  
304 some background in computer programming, we are working to provide a web version of ENQUIRE  
305 to ease its adoption among biomedical researchers.

306 **DATA AVAILABILITY**

307 ENQUIRE's main program and the standalone scripts to perform the *post hoc* analyses are included in  
308 an Apptainer/Singularity image file (SIF), available for download at  
309 <https://figshare.com/articles/software/ENQUIRE/24434845> (DOI:  
310 10.6084/m9.figshare.24434845.v3). Installation and running instructions, gene-symbol-to-alias lookup  
311 table, input and output files from the exemplary case study, and data underlying the results (**Supp.**  
312 **Information**) can be found at <https://github.com/Muszeb/ENQUIRE> (DOI:  
313 10.5281/zenodo.10692274). All the individual scripts are also available upon request.

314 **AUTHOR CONTRIBUTIONS**

315 Idea and concept: LM and JV. Coding and benchmarking of the algorithm: LM and MW. Drafting of  
316 the manuscript: LM, XL, and JV. All the authors edited, corrected, and approved the submitted draft.

317 **ACKNOWLEDGEMENTS**

318 We thank Martin Eberhardt, Christopher Lischer, Jimmy Retzlaff, Esther Güse, and Suryadipto Sarkar  
319 for the useful scientific discussions, comments on the manuscript, and testing the installation and  
320 running of the algorithm.

321 **FUNDING**

322 This work has been supported by the German Ministry of Education and Science (BMBF) thorough  
323 the projects e:Med MelAutim and KI-VesD I and II. XL acknowledges the support from the Johannes  
324 and Frieda Marohn Foundation.

325

326 **MATERIALS AND METHODS**

327 **Description of the ENQUIRE algorithm**

328 **Extraction of Article Metadata**

329 ENQUIRE uses the NCBI's e-utilities to query and fetch information from the PubMed database<sup>59</sup>.  
330 *Epost* is used to request a collection of PMIDs, *efetch* to extract their metadata in XML format, and  
331 *esearch* to construct PubMed queries.

332 **MeSH Term and Article Abstract Extraction**

333 For each MEDLINE-indexed, input PMID, if the MeSH entity scope is selected, ENQUIRE retrieves  
334 MeSH main headings (“descriptors”) and subheadings (“qualifiers”) from their respective *efetch*-  
335 retrieved XML files. These MeSH terms are further selected to match biomedically relevant, non-  
336 redundant categories, by exploiting the tree-like, hierarchical structure of the MeSH vocabulary. By  
337 default, ENQUIRE only retains members downstream of the MeSH categories A (Anatomy), C  
338 (Diseases), D (Chemicals and Drugs), and G (Phenomena and Processes), except for sub-categories  
339 G01 (Physical Phenomena), G02 (Chemical Phenomena) and G17 (Mathematical Concepts).

340 **Gene Normalization from Article Abstracts**

341 For each input PMID, if the gene entity scope is selected, ENQUIRE retrieves article abstracts from  
342 their respective *efetch*-retrieved XML files. As other authors have shown that the proportion of gene  
343 mentions does not significantly differ between abstracts and full-body texts<sup>60</sup>, we only mine the  
344 abstracts for gene mentions. In contrast to standard named entity recognition of genes (NER), whose  
345 task is to exactly match the character span of a gene mention, ENQUIRE's textmining framework aims  
346 at detecting least one gene alias per unique reference gene mentioned in an abstract. We therefore  
347 designed a “Swiss cheese model” for gene normalization, in which multiple methods complement each  
348 other to improve the global precision. In brief, ENQUIRE applies up to two algorithms to each  
349 unprocessed abstract: i) the Schwartz-Hearst algorithm to detect single-word abbreviations and their  
350 respective definitions<sup>33</sup>; ii) the optional scispaCy model (*en\_ner\_jnlpba\_md*) to identify words  
351 classified as “CELL\_LINE” or “CELL\_TYPE”<sup>34</sup>. This allows ENQUIRE to construct abstract-specific  
352 blocklists that discard i) ambiguous abbreviations whose definitions are not similar to any gene alias  
353 from a pre-annotated lookup table, and ii) ambiguous or unwanted mentions to cell entities containing  
354 gene aliases, such as “CD8+ T cell”. Finally, a tokenization module generates potential gene-alias-  
355 matching tokens and redirects them to a unique, reference gene symbol using the lookup table.

356 **Construction of the Lookup Table of Reference Gene Names and Respective Aliases**

357 Similar to previous approaches<sup>61</sup>, ENQUIRE performs NER of *Homo sapiens* and *Mus musculus* gene  
358 mentions, while also redirecting the latter to their respective human homologues using MGI's  
359 mouse/human orthology table<sup>62</sup>. Each reference gene name corresponds to HGNC approved symbol<sup>63</sup>.  
360 Additional mouse and human gene aliases were pooled from HGNC (“previous symbols”, “previous  
361 names”, “alias symbols”, “alias names”), ENSEMBL (“gene stable ID”, “gene description”, “gene  
362 name”), Uniprot (“gene names”, “protein names”), and miRBase (“ID”, “alias”, “name”)<sup>64-66</sup>. We  
363 manually inspected sources of ambiguities and lack of spelling variants: for example, we added  
364 miRNA names without species suffixes (e.g. “miR-335” from “hsa-miR-335”), multiple spellings for  
365 lnc- and mi-RNAs (e.g. “LNC/Lnc/lnc”, “miR/mir”) and removed aliases identical to common

366 acronyms for experimental techniques (e.g. “MRI”, “NMR”, “TEM”). We converted Greek letters to  
367 their literal spelling. We resolved ambiguities due to aliases reported under more than one reference  
368 symbol, by either assigning the alias to a single reference, or by excluding the alias.

369 **Abstract Tokenization for Named-Entity Recognition of Genes**

370 ENQUIRE mostly performs named-entity recognition of genes (NER) from article abstracts by exact  
371 matches between gene aliases and space- or punctuation-separated word tokens. We exclude general-  
372 purpose English words annotated in the *English-words* Python library to reduce the computational  
373 burden of mapping gene mentions. Greek letters are converted to their literal spelling. Special attention  
374 is put to hyphen- and slash-containing tokens, tracing their usage as integral parts of gene aliases (e.g.  
375 “TNF-alpha”) or separators (e.g. “FcγR-TLR Cross-Talk” – PMID 31024565, “Akt/PI3K/mTOR  
376 signaling pathway” – PMID 35802302). When cases of the latter kind occur, the algorithm requires all  
377 hyphen- or slash-separated words to be gene aliases, in order to be considered individual tokens. Then,  
378 ENQUIRE tokenizes the abstract into single-word tokens and interprets unambiguous tokens as the  
379 corresponding reference gene symbol if they match an alias in the lookup table. Multiple mentions of  
380 the same gene within an abstract count as one.

381 **Abstract-Specific Blocklists Using Cell Entity Mentions and Abbreviation-Definition Pairs**

382 Any token that exactly matches an alias from the lookup table is redirected to the respective reference  
383 symbol, except when that same token is either classified as part of “CELL\_LINE” or “CELL\_TYPE”  
384 entities, or as an abbreviation, by scispaCy *en\_ner\_jnlpba\_md* and Schwartz-Hearst models. In the  
385 former exception, the token is added to a blocklist and any of its mentions within the abstract text are  
386 excluded from further gene normalization steps. In the latter exception, we evaluate the validity of an  
387 alias-matching abbreviation by means of its definition, as inferred by Schwartz-Hearst. We perform  
388 string comparison to calculate alignment scores between the definition and any recorded alias of the  
389 same reference symbol matched by the abbreviation. To this end, we implemented the Needleman-  
390 Wunsch algorithm for global alignment, with match score equal to 1, gap opening and mismatch  
391 penalties equal to -1, and gap extension penalty equal to -0.5<sup>67</sup>. Next, we calibrated a threshold for  
392 either retaining or discarding an alias-matching abbreviation according to its optimal alignment score.  
393 We used a dataset of abbreviation-description pairs from more than 300 abstracts and generated a  
394 distribution of scores by aligning any description to any annotated alias. Intuitively, there could only  
395 be a handful of alignments between an actual gene description and the aliases referring to that same  
396 gene, as opposed to several alignments between that same description and unrelated aliases. Therefore,  
397 we treated the above derived distribution as a model describing false positive alignments between  
398 descriptions and gene aliases. Finally, we identified a range between 0.1 and 0.2 that respectively  
399 correspond to 95th and 99th percentiles of the distribution of alignment scores as a sensible interval  
400 for choosing the threshold. We opted for a threshold of 0.15. Therefore, for any description whose  
401 abbreviation matches a gene alias, ENQUIRE records a gene mention only if the maximal alignment  
402 score against any alias of that same gene is higher or equal to this threshold; else, the abbreviation is  
403 added to the blocklist and all of its mentions within the text are excluded. Notice that the blocklist is  
404 independently computed for each abstract, thus making ENQUIRE’s gene normalization moderately  
405 adaptive with respect to syntactical context.

406 **Annotation and Weighting of Co-Occurrences**

407 ENQUIRE records the occurrences of MeSH and gene entities within each input article. Then, it counts  
408 pairwise co-occurrences by enumerating the subset of PMIDs associated to both entities in each pair.  
409 For each pair of entities  $g_i$  and  $g_j$  that co-occur in at least one article, we define the weights  $w$  and  
410 distances  $\tilde{w}$  accounting for the sheer co-occurrence  $X(g_i, g_j)$  as follows:

$$411 \quad 412 \quad w_{g_i, g_j} := \Psi(X(g_i, g_j), \bar{X}), \quad w_{g_i, g_j} \in (0, 1] \\ 413 \quad \tilde{w}_{g_i, g_j} = 1 - w_{g_i, g_j} \\ 414 \quad X(g_i, g_j) = |\{P \mid g_i, g_j \in E^P\}_{P \in \text{PMIDS}}|$$

415  
416 Where  $\bar{X}$  is the mean co-occurrence between any two entities in the corpus,  $\Psi(\cdot, \bar{X})$  is the zero-  
417 truncated, Poisson cumulative density function with a lambda of  $\bar{X}$ , and  $E^P$  is the set of all entities  
418 annotated within the PMID  $P$  that belongs to the submitted PMIDS corpus. This scoring system  
419 assigns higher relevance to co-occurrences that appear more often than average.

## 420 Reconstruction of a Weighted Network of Significant Co-Occurrences

421 ENQUIRE converts the recorded co-occurrences into an undirected multi-graph, where gene or MeSH  
422 terms become nodes, and each recorded co-occurrence between two entities becomes an edge. Thus,  
423 the network has as many nodes as the number of unique MeSH and gene symbols, with as many edges  
424 between two nodes as the number of PMIDs in which they co-occur. ENQUIRE implements the  
425 Casiraghi-Nanumyan's soft-configuration model applied to undirected, unweighted edge counts to  
426 select significant co-occurrences among entities, adjusted to 1% FDR<sup>21</sup>. The test statistics follows a  
427 multivariate hypergeometric distribution, under the null hypothesis of observing a random graph whose  
428 expected degree sequence correspond to the observed one. This allows us to condition the testing to  
429 the sheer, per-entity occurrence, which serves as a proxy for leveraging literature biases in the corpus.  
430 It is important to note that the null model does not assume independence of individual edges, but merely  
431 their equiprobability, and is unaffected by the weights  $w$ . This selection results in an undirected, single  
432 node-to-node edge co-occurrence graph (i.e. a simple graph). For each pair of adjacent entities  $g_i$  and  
433  $g_j$  in the simple network, we assign the weights  $w_{g_i, g_j}$  and distances  $\tilde{w}_{g_i, g_j}$  to their mutual edge.  
434 Additionally, we prune poorly connected nodes by modularity-based,  $w$ -weighted Leiden clustering<sup>68</sup>  
435 and removal of communities that consist of a single node. From the resulting gene/MeSH network, we  
436 also extract the respective gene- and MeSH-only subnetworks.  
437 ENQUIRE-generated gene/MeSH networks can consist of multiple connected components, i.e.  
438 subgraphs. To exclude unimportant components, a subgraph  $S$  is retained for subsequent computations  
439 only if the fraction of corpus articles covered by  $S$  is higher than a threshold value, as formally defined  
440 in

$$442 \quad T_S := \frac{|\{P \mid E^P \cap E^S \neq \emptyset\}_{P \in \text{PMIDS}}|}{|\text{PMIDS}|} \geq t, \quad T_S \in (0, 1]$$

443  
444 where  $P$  denotes a PMID belonging to PMIDS, and  $E^P$  and  $E^S$  refer to the sets of gene or MeSH  
445 entities recorded in either  $P$  or  $S$ . Therefore,  $T_S$  reflects the representativeness of  $S$  with respect to the  
446 entirety of the submitted corpus. The value of  $t$  can be set by the user. To avoid introducing irrelevant  
447 entities, ENQUIRE stops without further network expansion if the gene/MeSH network and the  
448 respective gene- and MeSH-only subnetworks individually contain only a single, connected

449 component with  $T_S \geq t$ . We compute the weight of a node  $g$  in the connected graph  $S$  utilizing the  
450 composite function  $W$ , which is the product of normalized metrics for betweenness centrality ( $b$ ) and  
451  $w$ -weighted degree strength ( $d$ ):  
452

$$453 \quad W(g, S) := F_b(b(g, S)) \cdot F_d(d(g, S)), \quad W \in (0, 1]$$

454

455 Here,  $F_x$  denotes the empirical cumulative density function for the corresponding  $x$  parameter,  
456 calculated over  $S$ .

## 457 Construction of Communities from “Information-Dense” Cliques

458 To identify the most relevant parts of the gene/MeSH network, ENQUIRE first identifies the maximal  
459 cliques of order three or more. By definition, these are graphlets whose nodes are all adjacent to each  
460 other and not a subset of a larger clique. Applying the KNet function from the SANTA R package<sup>40</sup> to  
461 the gene/MeSH network having distances  $\tilde{w}_{g_i, g_j}$ , we select cliques that form significant clusters of  
462 associated entities. The permutation test procedure internal to KNet allows us to consider the network  
463 topology and adjust each maximal clique’s significance, in case many other cliques of similar size exist  
464 in the network. We set the significance level for this test to 1% FDR. Subsequently, ENQUIRE  
465 generates a pruned network  $C$  containing only statistically significant cliques. Here, ENQUIRE stops  
466 if the gene/MeSH network contains less than two significant cliques according to KNet. Next,  
467 ENQUIRE identifies communities in the  $C$  network using modularity-based,  $w$ -weighted Leiden  
468 clustering. ENQUIRE stops if it detects a single community that encompasses all nodes in  $C$ .

## 469 Identification of Community-Connecting Entities

470 For any two disjoint communities  $C_i$  and  $C_j$ , we select the set of community-connecting, weighted  
471 graphlets  $\Gamma_{C_i, C_j}(V_k, L_{k-1})$  satisfying the properties: i) all nodes  $g_i$  in the  $k$ -sized set  $V_k$  belong to either  
472  $C_i$  or  $C_j$ ; ii) the intersections between  $V_k$  and  $C_i$  or  $C_j$  are non-empty; iii) the  $w$ -weighted,  $k - 1$  edges  
473  $L_{k-1}$  are sufficient to obtain a single connected component; iv) there is only one edge  $l_{g_i, g_j}$  that  
474 connects nodes belonging to distinct communities. Here,  $k$  is a parameter chosen by the user.  
475 This allows us to rank the set of community-connecting entities  $V_k$  in any graphlet  $\Gamma_{C_i, C_j}$  by means of  
476 the distance metric  $R$ :  
477

$$478 \quad R\left(\Gamma_{C_i, C_j}(V_k, L_{k-1})\right) := -\log\left(\prod_{g_i \in V_k} W(g_i, \cdot) \prod_{l_{g_i, g_j} \in L_{k-1}} w_{g_i, g_j}\right), \quad R \in \mathbb{R}_{\geq 0}$$
$$479 \quad V_k \in C_i \cup C_j, V_k \cap C_i \neq \emptyset, V_k \cap C_j \neq \emptyset$$
$$480 \quad \left| \{l_{g_i, g_j} \mid g_i \in C_i, g_j \in C_j\}_{l_{g_i, g_j} \in L_{k-1}} \right| = 1$$

481 The smaller  $R$ , the closer two communities connected by  $V_k$  are.

## 483 Retrieval of New PMIDs via PubMed Queries Based on Optimal Connections

484 To evaluate which genes and MeSH terms are particularly suited for expansion querying, ENQUIRE  
485 constructs a multigraph  $M$  where network communities become nodes and all  $R$ -weighted connections  
486 between two communities become edges.  $R$ -weighted edges that do not fulfil the triangle inequality

487  $R(\Gamma_{C_i, C_j}) \leq R(\Gamma_{C_i, C_z}) + R(\Gamma_{C_z, C_j})$ ,  $\forall i, j, z$  are excluded. Then, we solve the travelling salesman  
488 problem (TSP) utilizing Christofides' approximate solution as implemented in the Python package  
489 Networkx<sup>69</sup>. Via the visited edges, this yields an optimal path across communities and a corresponding  
490 collection of  $V_k$  entity sets. Each selected  $k$ -sized set  $V_k$  results in a PubMed query formulated via the  
491 NCBI's *esearch* utility<sup>59</sup>. We condition the search terms representing gene aliases and MeSH with  
492 “[Title/Abstract]” and “[MeSH Terms]”, respectively, and exclude review articles from the results.  
493 The constructed PubMed queries require a match for all the  $k$  entities in the optimal path – e.g.  
494 “*melanoma/immunology*”[MeSH Terms] AND (“*IL1B*”[Title/Abstract] OR “*interleukin 1-beta*”[Title/Abstract] [...] AND [...]). If all queries involving a subset of the network communities  
495 lead to empty results, we prune all previously used edges from  $M$ , compute a new TSP solution, and  
496 submit newly generated queries, provided at least one entity per query belongs to such community  
497 subset. This process is repeated  $A$  times, where  $A$  is a parameter specified by the user. If at least 1 new  
498 PMID matches any of the constructed queries, ENQUIRE starts a new analysis from the union of new  
499 and old PMIDs; otherwise, it stops. The rationale behind merging old and new PMIDs is to account  
500 for the original corpus when computing the statistics on new co-occurrences.  
501

## 502 **Post-hoc Analyses**

### 503 **Context-Aware Gene Sets.**

504 To reconstruct contextual gene sets using gene/MeSH co-occurrence networks, we adapt network-  
505 based relational data to the method described by Khan *et al.*<sup>70</sup>. To this end, we first construct the inverse  
506 log-weighted similarity matrix between the gene/MeSH network nodes<sup>71</sup>. This metric prioritizes nodes  
507 sharing many lower degree neighbors rather than few higher degree ones. We derive a Euclidean  
508 distance matrix from the similarity matrix, after applying a Z-score standardization; then, we use the  
509 R package DynamicTreeCut and Ward's clustering to identify initial clusters and create an initial  
510 membership degree matrix<sup>72,73</sup>. Finally, we detect fuzzy clusters of genes and MeSH terms by applying  
511 Fuzzy C-means clustering to the Euclidean distance matrix, using the R package ppclust<sup>1,2</sup>. The  
512 resulting membership degree matrix allows annotating genes with desired cluster membership degrees  
513 and extracting the linked MeSH terms to characterize the gene set.

### 514 **Context-Aware Pathway Enrichment Analysis.**

515 We designed a method to map any text-mined co-occurrence network  $G$  onto a mechanistic reference  
516 network  $N$  and infer context-specific enrichment of molecular pathways. With this strategy, we  
517 attempt to mechanistically explain the indirect relationships that constitute the co-occurrence network.  
518 To this end, we define the fitness score  $Q$  for every gene  $g$  in  $N$  with non-zero node degree  $d$ :

519

$$520 Q(g) := d(g, N)^{-1} \cdot \sum_{g_i \in V(G)} \sum_{g_j \in V(G)} e^{-\tilde{\delta}_G(g_i, g_j)} \cdot \mathbb{1}_{\{\delta_N(g_i, g) + \delta_N(g, g_j) \leq 2, g_i \neq g_j\}}, \quad Q \in \mathbb{R}_{\geq 0}$$

521 Here,  $\tilde{\delta}_G(g_i, g_j)$  and  $\delta_N(g_i, g_j)$  are the  $\tilde{w}$ -weighted and unweighted distances from  $g_i$  to  $g_j$  in the  
522 graphs  $G$  and  $N$ , respectively. The indicator function  $\mathbb{1}$  implies that non-text-mined genes without at  
523 least two text-mined nodes as neighbors have  $Q$  equal to zero. We normalize all scores to decorrelate  
524  $Q$  from the node degree  $d$ , similarly to other approaches in network propagation<sup>74,75</sup>. As a mechanistic  
525 reference network, we chose STRING's (release 11.5) *H. sapiens* network of protein-coding,  
526

527 physically interacting genes<sup>38</sup>. We exclusively combined the “experimental” and “database” channels  
528 to calculate STRING’s confidence score, then pruned all edges with score below the 90<sup>th</sup> percentile.  
529 After removing zero-degree nodes, we obtain a reference, unweighted network of 9,482 nodes and  
530 88,333 edges. Then, we calculate  $Q$  scores for protein-coding genes in the STRING reference network  
531 ( $N$ ), using the ENQUIRE-generated gene network (G). We test for associations between predefined  
532 gene sets and high-scoring node clusters using SANTA’s KNet function<sup>40</sup>. KNet takes as input the  
533 STRING reference network, its nodes’  $Q$  scores, and a gene set; it then tests if the latter is enriched,  
534 based on scores and graph distances of protein-coding genes belonging to both the network and the  
535 gene set. This way, we aim at capturing known experimentally or database-derived molecular  
536 interactions relevant to ENQUIRE’s input literature corpus, using topology-based enrichment analysis.  
537 We test for enrichment on gene sets derived from Reactome pathways, obtained via the Reactome  
538 Graph database<sup>37</sup>. See **Supp. Fig. 2** for an example of  $Q$  score weighting.

539

## 540 **Benchmarks and Case Studies**

### 541 **Assessment of ENQUIRE's Gene Normalization Accuracy and Performance**

542 We evaluated ENQUIRE's gene normalization precision and recall using abstracts from the NLM-  
543 Gene corpus mentioning at least one *M. musculus* or *H. sapiens* gene – 479 out of 550 entries<sup>32</sup>. We  
544 tested the four module combinations obtained by either including or excluding the cell entity  
545 recognition module *en\_ner\_jnlpba\_md* and the *Schwartz-Hearst* abbreviation-definition algorithm<sup>33,34</sup>.  
546 We compared the computational performance of ENQUIRE's gene normalization method using both  
547 *en\_ner\_jnlpba\_md* and *Schwartz-Hearst* against GNorm2 implementation of Bioformer<sup>36,35</sup>. We  
548 computed wall time by accounting for both text processing and loading of required data such as gene  
549 alias lookup tables and machine learning models. RAM usage was measured using resident set size  
550 (RSS) measurements returned by the Linux built-in function *ps*. We ran the computations on a Linux  
551 computer with 20 CPUs (3.1 GHz) and 252 GB of RAM. Up to 8 cores were used for parallelization.

### 552 **Inference of Reactome Gene Sets from Reference Literature.**

553 We extracted annotated genes and reference literature for all *H. sapiens* Reactome pathways from the  
554 Reactome Graph database<sup>37</sup>. We employed NCBI's *esearch* and *elink* utilities to retrieve primary  
555 research articles cited by review articles<sup>59</sup>. After excluding pathways with less than three primary  
556 literature references or only one annotated human gene, we obtained a set of 967 pathways. For each  
557 pathway literature corpus, ENQUIRE performed one network reconstruction, set to only extract gene  
558 mentions from article abstracts. We evaluated the effects of corpus size, pathway size, and average  
559 gene-gene co-occurrence per abstract on precision and recall of ENQUIRE's gene normalization and  
560 network reconstruction. We also evaluated the correlation between true positives and the corpus- and  
561 network-based node weight  $W$ .

### 562 **Estimate of Molecular Interrelations.**

563 We automatically generated a list of case studies by crossing leaf nodes downstream of *Diseases* and  
564 *Genetic Phenomena* (G05) MeSH categories. We then constructed a PubMed query from each pair by  
565 “AND” concatenation. Examples of such queries are “*Stomach Neoplasm*”[MeSH Terms] AND  
566 “*Chromosomes, human, pair 18*”[MeSH Terms], and “*Acquired immunodeficiency syndrome*”[MeSH  
567 Terms] AND “*Polymorphism, single nucleotide*”[MeSH Terms]. For each query result with a size  
568 between 50 and 500 articles, we executed one network reconstruction. If obtaining a gene-gene co-  
569 occurrence network, we investigated whether its set of genes produced a network with more functional  
570 interactions than expected by chance. To obtain background distributions of edge counts for each gene  
571 set size observed with ENQUIRE, we sampled one million random gene sets and cumulated their  
572 interconnecting edges in STRING's v. 11.5 *H. sapiens* functional protein network. We only included  
573 functional associations from experiments, co-expression, and third-party databases with a cumulative  
574 score higher than 0.7 between proteins. The significance of each ENQUIRE-generated gene set's edge  
575 count was computed from the right-tailed probability of the empirical distribution.  
576 Moreover, we compared the ENQUIRE-generated gene-gene wirings to STRING-derived associations  
577 using the DeltaCon similarity measure in a permutation test<sup>39</sup>. To this end, we generated 10,000 random  
578 graphs for each observed ENQUIRE network. Each random graph was obtained through 300 random  
579 edge-swapping attempts while preserving the degree sequence of the original network. To obtain  
580 sensible probability densities, we focused on ENQUIRE-generated networks with degree sequences

581 allowing at least ten different realizations of a graph. We followed the formula  $\prod_i^n d_i!$ , where  $d_i$  is the  
582 degree of the  $i$ -th node of a graph containing  $n$  nodes.

583 **Assessment of Context Resolution by Topology-Based Enrichment of Molecular Pathways.**

584 To show that ENQUIRE preserves context-specific molecular signatures, we designed a broad panel  
585 of case studies (**Table 1**). Each corpus consisted of the union of references contained in three  
586 independent reviews accessible via NCBI's *elink* utility<sup>59</sup>. We selected reviews from the results of  
587 PubMed search queries consisting of two or three MeSH terms (e.g. “*Melanoma*”[MeSH Terms] AND  
588 “*Signal Transduction*”[MeSH Terms]), favoring PubMed-ranked best matches when possible. We also  
589 included an unspecific positive control group consisting of the union of all context-specific corpora.  
590 This experimental design allowed us to construct a reference dendrogram that clusters the case studies  
591 only based on baseline biological knowledge, expecting expanded networks of a case study to cluster  
592 together with the originally reconstructed one. Then, we applied ENQUIRE with default parameters to  
593 each case study and analyzed all resulting gene-gene networks, i.e., from original and expanded  
594 corpora. We computed pairwise similarities between node and edge sets of the constructed networks  
595 using Szymkiewicz-Simpson overlap coefficient (OC):  
596

$$597 \text{OC}(X,Y) = \frac{|X \cap Y|}{\min(|X|, |Y|)}, \quad \text{OC} \in [0,1]$$

598 Where  $X$  and  $Y$  are either two node sets or two edge sets. An OC of 0 indicates no overlap, while an  
599 OC of 1 indicates the smaller node or edge set is a subset of the larger one. By construction, same-  
600 case-study original and expanded networks possess OCs of 1 with each other. We applied the *post hoc*,  
601 context-aware pathway enrichment analysis described above to all generated networks. We tested the  
602 enrichment of Reactome pathways with sizes ranging from 3 to 100 genes, categorized as in the  
603 database's *Top-Level Pathways* and disease ontologies<sup>37</sup>. We performed hierarchical clustering of the  
604 networks using Euclidean distance and Kendall's correlation based on network-specific, KNet-  
605 generated p-values. We compared the resulting dendrogram to the expected one by a permutation test  
606 of Baker's gamma correlation using one million permutations of the original dendrogram<sup>45</sup>. We also  
607 compared the results to two alternative statistics: i) over-representation analysis of nodes from the  
608 ENQUIRE-generated networks (the collection of all genes observed in any case study was used as the  
609 “universe”); ii) KNet statistics, using  $Q$  scores based on STRING's high-confidence functional  
610 association network (described above) and ENQUIRE-derived gene nodes.  
611

612 REFERENCES

- 613 1. Vitali, F. *et al.* A network-based data integration approach to support drug repurposing and  
614 multi-Target therapies in triple negative breast cancer. *PLoS ONE* **11**, (2016).
- 615 2. Cantone, M. *et al.* A gene regulatory architecture that controls region-independent dynamics of  
616 oligodendrocyte differentiation. *Glia* **67**, 825–843 (2019).
- 617 3. Sadegh, S. *et al.* Network medicine for disease module identification and drug repurposing with  
618 the NeDREx platform. *Nat. Commun.* **12**, 6848 (2021).
- 619 4. Lai, X. *et al.* A disease network-based deep learning approach for characterizing melanoma. *Int.*  
620 *J. Cancer* **150**, 1029–1044 (2022).
- 621 5. Grimes, D. R. & Heathers, J. The new normal? Redaction bias in biomedical science. *R. Soc.*  
622 *Open Sci.* **8**, 211308 (2021).
- 623 6. Haynes, W. A., Tomczak, A. & Khatri, P. Gene annotation bias impedes biomedical research.  
624 *Sci. Rep.* **8**, 1362 (2018).
- 625 7. Tomczak, A. *et al.* Interpretation of biological experiments changes with evolution of the Gene  
626 Ontology and its annotations. *Sci. Rep.* **8**, 5115 (2018).
- 627 8. Ewing, E., Planell-Picola, N., Jagodic, M. & Gomez-Cabrero, D. GeneSetCluster: A tool for  
628 summarizing and integrating gene-set analysis results. *BMC Bioinformatics* **21**, (2020).
- 629 9. Kveler, K. *et al.* Immune-centric network of cytokines and cells in disease context identified by  
630 computational mining of PubMed. *Nat. Biotechnol.* **36**, 651–659 (2018).
- 631 10. Macnee, M. *et al.* SimText: A text mining framework for interactive analysis and visualization of  
632 similarities among biomedical entities. *Bioinforma. Oxf. Engl.* **37**, 4285–7 (2021).
- 633 11. Luo, L. *et al.* AIONER: all-in-one scheme-based biomedical named entity recognition using deep  
634 learning. *Bioinformatics* **39**, btad310 (2023).

635 12. Chen, D. & Manning, C. A Fast and Accurate Dependency Parser using Neural Networks. in  
636 *Proceedings of the 2014 Conference on Empirical Methods in Natural Language Processing*  
637 (*EMNLP*) 740–750 (Association for Computational Linguistics, Stroudsburg, PA, USA, 2014).  
638 doi:10.3115/v1/D14-1082.

639 13. Miao, Q., Zhang, S., Meng, Y., Fu, Y. & Yu, H. Healthy or Harmful? Polarity Analysis Applied  
640 to Biomedical Entity Relationships. in 777–782 (2012). doi:10.1007/978-3-642-32695-0\_72.

641 14. Junge, A. & Jensen, L. J. CoCoScore: context-aware co-occurrence scoring for text mining  
642 applications using distant supervision. *Bioinformatics* **36**, 264–271 (2020).

643 15. Lee, J. *et al.* BioBERT: a pre-trained biomedical language representation model for biomedical  
644 text mining. *Bioinformatics* **36**, 1234–1240 (2020).

645 16. Islam, M. R., Liu, S., Wang, X. & Xu, G. Deep learning for misinformation detection on online  
646 social networks: a survey and new perspectives. *Soc. Netw. Anal. Min.* **10**, 82 (2020).

647 17. Diaz-Garcia, J. A., Fernandez-Basso, C., Ruiz, M. D. & Martin-Bautista, M. J. Mining Text  
648 Patterns over Fake and Real Tweets. in *Information Processing and Management of Uncertainty*  
649 *in Knowledge-Based Systems* (eds. Lesot, M.-J. *et al.*) 648–660 (Springer International  
650 Publishing, Cham, 2020).

651 18. Ioannidis, J. P. A. Why Most Published Research Findings Are False. *PLoS Med.* **2**, e124 (2005).

652 19. Baker, M. 1,500 scientists lift the lid on reproducibility. *Nature* **533**, 452–454 (2016).

653 20. HAYNES, W. A. *et al.* EMPOWERING MULTI-COHORT GENE EXPRESSION ANALYSIS  
654 TO INCREASE REPRODUCIBILITY. in *Biocomputing 2017* 144–153 (WORLD SCIENTIFIC,  
655 2017). doi:10.1142/9789813207813\_0015.

656 21. Casiraghi, G. & Nanumyan, V. Configuration models as an urn problem. *Sci. Rep.* **11**, 13416  
657 (2021).

658 22. Andres, G., Casiraghi, G., Vaccario, G. & Schweitzer, F. Reconstructing signed relations from  
659 interaction data. *Sci. Rep.* **13**, 20689 (2023).

660 23. Dang, Q. *et al.* Ferroptosis: a double-edged sword mediating immune tolerance of cancer. *Cell*  
661 *Death Dis.* **13**, 925 (2022).

662 24. Shannon, P. *et al.* Cytoscape: a software environment for integrated models of biomolecular  
663 interaction networks. *Genome Res.* **13**, 2498–2504 (2003).

664 25. Goenawan, I. H., Bryan, K. & Lynn, D. J. DyNet: visualization and analysis of dynamic  
665 molecular interaction networks. *Bioinformatics* **32**, 2713–2715 (2016).

666 26. Li, W. *et al.* Ferroptotic cell death and TLR4/Trif signaling initiate neutrophil recruitment after  
667 heart transplantation. *J. Clin. Invest.* **129**, 2293–2304 (2019).

668 27. Lang, X. *et al.* Radiotherapy and Immunotherapy Promote Tumoral Lipid Oxidation and  
669 Ferroptosis via Synergistic Repression of SLC7A11. *Cancer Discov.* **9**, 1673–1685 (2019).

670 28. Tang, X. *et al.* Curcumin induces ferroptosis in non-small-cell lung cancer via activating  
671 autophagy. *Thorac. Cancer* **12**, 1219–1230 (2021).

672 29. Quagliariello, V. *et al.* The SGLT-2 inhibitor empagliflozin improves myocardial strain, reduces  
673 cardiac fibrosis and pro-inflammatory cytokines in non-diabetic mice treated with doxorubicin.  
674 *Cardiovasc. Diabetol.* **20**, 150 (2021).

675 30. Li, Y. *et al.* MGST1 Expression Is Associated with Poor Prognosis, Enhancing the Wnt/β-  
676 Catenin Pathway via Regulating AKT and Inhibiting Ferroptosis in Gastric Cancer. *ACS Omega*  
677 **8**, 23683–23694 (2023).

678 31. Nakamura, T. *et al.* Phase separation of FSP1 promotes ferroptosis. *Nature* **619**, 371–377 (2023).

679 32. Islamaj, R. *et al.* NLM-Gene, a richly annotated gold standard dataset for gene entities that  
680 addresses ambiguity and multi-species gene recognition. *J. Biomed. Inform.* **118**, 103779 (2021).

681 33. Schwartz, A. S. & Hearst, M. A. A Simple Algorithm for Identifying Abbreviation Definitions in  
682 Biomedical Text. *Pac. Symp. Biocomput. Pac. Symp. Biocomput.* 451–62 (2002).

683 34. Neumann, M., King, D., Beltagy, I. & Ammar, W. ScispaCy: Fast and Robust Models for  
684 Biomedical Natural Language Processing. in *Proceedings of the 18th BioNLP Workshop and*  
685 *Shared Task* 319–327 (Association for Computational Linguistics, Stroudsburg, PA, USA,  
686 2019). doi:10.18653/v1/W19-5034.

687 35. Wei, C.-H., Luo, L., Islamaj, R., Lai, P.-T. & Lu, Z. GNorm2: an improved gene name  
688 recognition and normalization system. *Bioinformatics* **39**, btad599 (2023).

689 36. Fang, L., Chen, Q., Wei, C.-H., Lu, Z. & Wang, K. Bioformer: an efficient transformer language  
690 model for biomedical text mining. <https://arxiv.org/abs/2302.01588> (2023).

691 37. Fabregat, A. *et al.* Reactome graph database: Efficient access to complex pathway data. *PLOS*  
692 *Comput. Biol.* **14**, e1005968- (2018).

693 38. Szklarczyk, D. *et al.* The STRING database in 2021: customizable protein–protein networks, and  
694 functional characterization of user-uploaded gene/measurement sets. *Nucleic Acids Res.* **49**,  
695 D605–D612 (2021).

696 39. Koutra, D., Shah, N., Vogelstein, J. T., Gallagher, B. & Faloutsos, C. DeltaCon: Principled  
697 Massive-Graph Similarity Function with Attribution. *ACM Trans Knowl Discov Data* **10**, (2016).

698 40. Cornish, A. J. & Markowetz, F. SANTA: Quantifying the Functional Content of Molecular  
699 Networks. *PLOS Comput. Biol.* **10**, e1003808- (2014).

700 41. Tikoo, R. *et al.* Ectopic expression of p27Kip1 in oligodendrocyte progenitor cells results in cell-  
701 cycle growth arrest. *J. Neurobiol.* **36**, 431–440 (1998).

702 42. Nygård, M., Wahlström, G. M., Gustafsson, M. V., Tokumoto, Y. M. & Bondesson, M.  
703 Hormone-Dependent Repression of the E2F-1 Gene by Thyroid Hormone Receptors. *Mol.*  
704 *Endocrinol.* **17**, 79–92 (2003).

705 43. Magri, L. *et al.* E2F1 Coregulates Cell Cycle Genes and Chromatin Components during the  
706 Transition of Oligodendrocyte Progenitors from Proliferation to Differentiation. *J. Neurosci.* **34**,  
707 1481 (2014).

708 44. Jaiswal, M. *et al.* Clinical Correlation and Role of Cyclin D1 Expression in Glioblastoma  
709 Patients: A Study From North India. *Cureus* **14**, e22346–e22346 (2022).

710 45. Baker, F. B. Stability of Two Hierarchical Grouping Techniques Case 1: Sensitivity to Data  
711 Errors. *J. Am. Stat. Assoc.* **69**, 440–445 (1974).

712 46. Wei, C.-H., Allot, A., Leaman, R. & Lu, Z. PubTator central: automated concept annotation for  
713 biomedical full text articles. *Nucleic Acids Res.* **47**, W587–W593 (2019).

714 47. Sung, M. *et al.* BERN2: an advanced neural biomedical named entity recognition and  
715 normalization tool. *Bioinformatics* **38**, 4837–4839 (2022).

716 48. Xiang, Z., Qin, T., Qin, Z. S. & He, Y. A genome-wide MeSH-based literature mining system  
717 predicts implicit gene-to-gene relationships and networks. *BMC Syst. Biol.* **7**, S9 (2013).

718 49. Kim, J. *et al.* DigSee: disease gene search engine with evidence sentences (version cancer).  
719 *Nucleic Acids Res.* **41**, W510–W517 (2013).

720 50. Kim, J. *et al.* IMA: Identifying disease-related genes using MeSH terms and association rules. *J.*  
721 *Biomed. Inform.* **76**, 110–123 (2017).

722 51. Nam, Y. *et al.* The translational network for metabolic disease – from protein interaction to  
723 disease co-occurrence. *BMC Bioinformatics* **20**, 576 (2019).

724 52. Marra, M., Emrouznejad, A., Ho, W. & Edwards, J. S. The value of indirect ties in citation  
725 networks: SNA analysis with OWA operator weights. *Inf. Sci.* **314**, 135–151 (2015).

726 53. Han, X., Shen, Z., Wang, W.-X., Lai, Y.-C. & Grebogi, C. Reconstructing direct and indirect  
727 interactions in networked public goods game. *Sci. Rep.* **6**, 30241 (2016).

728 54. Mei, S., Flemington, E. K. & Zhang, K. A computational framework for distinguishing direct  
729 versus indirect interactions in human functional protein–protein interaction networks. *Integr.*  
730 *Biol.* **9**, 595–606 (2017).

731 55. Hawe, J. S., Theis, F. J. & Heinig, M. Inferring Interaction Networks From Multi-Omics Data.  
732 *Front. Genet.* **10**, (2019).

733 56. Xiao, N. *et al.* Disentangling direct from indirect relationships in association networks. *Proc.*  
734 *Natl. Acad. Sci. U. S. A.* **119**, e2109995119 (2022).

735 57. Nguyen, D. Q. & Verspoor, K. From POS tagging to dependency parsing for biomedical event  
736 extraction. *BMC Bioinformatics* **20**, 72 (2019).

737 58. Szklarczyk, D. *et al.* STRING v11: protein-protein association networks with increased coverage,  
738 supporting functional discovery in genome-wide experimental datasets. *Nucleic Acids Res.* **47**,  
739 D607–D613 (2019).

740 59. Kans, J. *Entrez Direct: E-Utilities on the Unix Command Line.*  
741 <https://www.ncbi.nlm.nih.gov/books/NBK179288/> (2013).

742 60. Cohen, K. B., Johnson, H. L., Verspoor, K., Roeder, C. & Hunter, L. E. The structural and  
743 content aspects of abstracts versus bodies of full text journal articles are different. *BMC*  
744 *Bioinformatics* **11**, 492 (2010).

745 61. Pyysalo, S. *et al.* LION LBD: a literature-based discovery system for cancer biology.  
746 *Bioinformatics* **35**, 1553–1561 (2019).

747 62. Ringwald, M. *et al.* Mouse Genome Informatics (MGI): latest news from MGD and GXD.  
748 *Mamm. Genome* **33**, 4–18 (2022).

749 63. Seal, R. L. *et al.* Genenames.org: the HGNC resources in 2023. *Nucleic Acids Res.* **51**, D1003–  
750 D1009 (2023).

751 64. Martin, F. J. *et al.* Ensembl 2023. *Nucleic Acids Res.* **51**, D933–D941 (2023).

752 65. Consortium, T. U. UniProt: the Universal Protein Knowledgebase in 2023. *Nucleic Acids Res.*  
753 **51**, D523–D531 (2023).

754 66. Kozomara, A., Birgaoanu, M. & Griffiths-Jones, S. miRBase: from microRNA sequences to  
755 function. *Nucleic Acids Res.* **47**, D155–D162 (2019).

756 67. Needleman, S. B. & Wunsch, C. D. A general method applicable to the search for similarities in  
757 the amino acid sequence of two proteins. *J. Mol. Biol.* **48**, 443–453 (1970).

758 68. Traag, V. A., Waltman, L. & van Eck, N. J. From Louvain to Leiden: guaranteeing well-  
759 connected communities. *Sci. Rep.* **9**, 5233 (2019).

760 69. Hagberg, A., Swart, P. J. & Schult, D. A. Exploring network structure, dynamics, and function  
761 using NetworkX. in (United States, 2008).

762 70. Khan, A., Katanic, D. & Thakar, J. Meta-analysis of cell- specific transcriptomic data using  
763 fuzzy c-means clustering discovers versatile viral responsive genes. *BMC Bioinformatics* **18**, 295  
764 (2017).

765 71. Adamic, L. A. & Adar, E. Friends and neighbors on the Web. *Soc. Netw.* **25**, 211–230 (2003).

766 72. Ward, J. H. Hierarchical Grouping to Optimize an Objective Function. *J. Am. Stat. Assoc.* **58**,  
767 236–244 (1963).

768 73. Langfelder, P., Zhang, B. & Horvath, S. Defining clusters from a hierarchical cluster tree: the  
769 Dynamic Tree Cut package for R. *Bioinformatics* **24**, 719–720 (2008).

770 74. Bello, T. *et al.* KiRNet: Kinase-centered network propagation of pharmacological screen results.  
771 *Cell Rep. Methods* **1**, 100007 (2021).

772 75. Crowl, S., Jordan, B. T., Ahmed, H., Ma, C. X. & Naegle, K. M. KSTAR: An algorithm to  
773 predict patient-specific kinase activities from phosphoproteomic data. *Nat. Commun.* **13**, 4283  
774 (2022).

775

776 **TABLES**

777 **Table 1. Selection of case studies for assessment of context resolution at the molecular pathway**  
778 **level.** We obtained PubMed queries by “AND” concatenation of up to three MeSH terms and further  
779 filters to retrieve review articles only. The Corpus sizes refer to the non-redundant union of  
780 publications cited by three independent review articles, reported under the “References” column.

Major Topic	Case Study (abbreviation)	PubMed Query			Corpus size	References (PMID)
		MeSH 1	MeSH 2	MeSH 3		
Signal transduction in solid tumors	<b>Melanoma (MM-ST)</b>	Signal transduction	Melanoma		944	25587943, 32605090, 34924562
	<b>Uveal melanoma (UM-ST)</b>	Signal transduction	Uveal neoplasms		218	25296731, 25113308, 28223438
	<b>Colorectal cancer (COL)</b>	Signal transduction	Colorectal neoplasms		556	34884633, 34742312, 35836256
	<b>Breast cancer (BRE-ST)</b>	Signal transduction	Breast neoplasms		522	29455658, 31752925, 32245065
Macrophage's signal transduction in disease	<b>Macrophage signal transduction upon infection (MP-ST)</b>	Signal transduction	Macrophages	Mycobacterium tuberculosis	470	32849525, 33558322, 34502407
	<b>Tumor-associated Macrophages (MP-TA)</b>	Signal transduction	Tumor associated macrophages		386	33365025, 35844605, 35740975
Antigen presentation in autoimmune diseases	<b>Inflammatory bowel disease (IBD-AP)</b>	Antigen presentation	Inflammatory bowel diseases		445	28534191, 33584726, 33800865
	<b>Rheumatoid arthritis (RA_AP)</b>	Antigen presentation	Arthritis, rheumatoid		452	27225300, 28451787, 30589082
	<b>Psoriasis (PSO-AP)</b>	Antigen presentation	Psoriasis		435	26215033, 29316717, 33050592
Oligodendrocyte differentiation	<b>Oligodendrocyte (ODC)</b>	Cell differentiation	Oligodendroglia		355	24979526, 30770136, 31614602
Positive control	<b>All case studies (CTR)</b>	All queries (“OR” concatenation)			3606	All of the above

781

782 **Table 2. Performance of ENQUIRE's gene normalization algorithm.** The gene normalization task  
783 is here defined as detecting at least one gene alias per unique reference gene mentioned in an abstract.  
784 Precision, recall, and their harmonic mean (F1) are based on annotated abstracts from the NLM-Gene  
785 corpus containing at least one mention to a *H. sapiens* or *M. musculus* gene (479 abstracts). We ran the  
786 computations on a Linux computer with 20 CPUs (3.1 GHz) and 252 GB of RAM. Up to 8 cores were  
787 used for parallelization. We tested different gene normalization methods by adding or removing filters  
788 for excluding predicted cell entities (*en\_ner\_jnlpba\_md*) and ambiguous abbreviation-definition pairs  
789 (Schwartz-Hearst). Maximum RAM usage is measured as resident set size (RSS). Estimated time in  
790 seconds per abstract (sec/abstract) also accounts for loading the gene alias lookup table and machine  
791 learning models. The best value for each parameter setting is highlighted in bold.

Gene normalization Method	Precision	Recall <sup>1</sup>	F1	Computing performance			
				Resource usage	Cores		
					1	4	8
<i>en_ner_jnlpba_md</i> + Schwartz-Hearst + ENQUIRE tokenizer/dictionary	<b>0.823</b>	0.662	0.734	Max. RSS (GB)	1.95	1.95	1.95
				sec/abstract	0.172	0.0656	0.0488
Schwartz-Hearst + ENQUIRE tokenizer/dictionary	0.822	0.683	<b>0.747</b>	Max. RSS (GB)	<b>0.359</b>	<b>0.359</b>	0.361
				sec/abstract	0.125	0.0435	0.0318
<i>en_ner_jnlpba_md</i> + ENQUIRE tokenizer/dictionary	0.804	0.666	0.728	Max. RSS (GB)	1.95	1.95	1.95
				sec/abstract	0.148	0.0651	0.0481
ENQUIRE tokenizer/dictionary	0.802	<b>0.688</b>	0.741	Max. RSS (GB)	0.360	<b>0.359</b>	<b>0.359</b>
				sec/abstract	<b>0.105</b>	<b>0.0400</b>	<b>0.0280</b>

792

<sup>1</sup>Gene mentions contained in cell entities such as “CD8+ T cell” are true positives in the NLM-Gene corpus. Text spans tagged as cell entities by the *en\_ner\_jnlpba* model are removed without being processed by the tokenizer module, affecting recall.

793  
794 **Table 3. Differences in computing performance between ENQUIRE's gene normalization**  
795 **algorithm and GNorm2-Bioformer.** We ran the computations on a Linux computer with 20 CPUs  
796 (3.1 GHz) and 252 GB of RAM. Up to 8 cores were used for parallelization. Maximum RAM usage  
797 was measured as resident set size (RSS). Estimated time in seconds per process abstract (sec/abstract)  
also accounts for loading of gene alias lookup table and machine learning models.

Gene normalization method	Corpus size	Computing performance			
		Resource usage	Threads		
			1	4	8
<i>en_ner_jnlpba_md + Schwartz-Hearst + ENQUIRE tokenizer/dictionary</i>	26	<b>Max. RSS (GB)</b>	1.95	1.95	1.95
		<b>sec/abstract</b>	0.573	0.509	0.513
<b>GNorm2-Bioformer</b>		<b>Max. RSS (GB)</b>	17.3	16.4	17.4
		<b>sec/abstract</b>	4.310	4.150	2.73
<i>en_ner_jnlpba_md + Schwartz-Hearst + ENQUIRE tokenizer/dictionary</i>	130	<b>Max. RSS (GB)</b>	2.08	1.95	1.95
		<b>sec/abstract</b>	0.205	0.134	0.125
<b>GNorm2-Bioformer</b>		<b>Max. RSS (GB)</b>	25.1	25.1	24.7
		<b>sec/abstract</b>	2.500	1.260	1.070
<i>en_ner_jnlpba_md + Schwartz-Hearst + ENQUIRE tokenizer/dictionary</i>	1300	<b>Max. RSS (GB)</b>	5.9	2.91	2.71
		<b>sec/abstract</b>	0.118	0.044	0.030
<b>GNorm2-Bioformer</b>		<b>Max. RSS (GB)</b>	25.0	24.8	24.9
		<b>sec/abstract</b>	2.370	1.050	0.835

798

799 **Table 4. Effect of relevant covariates on quality indicators of ENQUIRE's gene entity**  
800 **recognition.** We evaluated the effect of corpus size (input), Reactome's pathway size (number of genes  
801 to be retrieved) and average gene-gene co-occurrence per article, using Spearman's correlation  
802 coefficients, for each measure. FPR: false positive rate.

Metric	Corpus Size	Pathway Size	Average co-occurrence
<b>Precision</b>	-0.18	0.49	-0.06
<b>Recall</b>	0.46	-0.35	0.14

803

804 **Table 5. Relevant quality indicators of functional associations in 3098 case studies.** PPI: protein-  
805 protein interaction score, as number of observed edges over the STRING-inferred network. FDR: false  
806 discovery rate, expressed in percentage. Percentages reported for PPI and DeltaCon significance  
807 independently refer to the set of 733 tested networks, i.e. those with 10 or more possible realizations  
808 with the same degree sequence as ENQUIRE-derived networks.

Property	Subset	Raw count	Percentage over the preceding step	Percentage over total (3098)
Network topology	<b>At least 3 genes and 2 edges in both ENQUIRE and STRING networks</b>	1336	/	43.1%
	<b>At least 10 possible realizations of the same degree sequence</b>	733	54.9%	23.7%
Significance	<b>Edge count p-value</b>	< 0.05	730	99.6%
		< 1% FDR	722	98.5%
	<b>DeltaCon p-value</b>	< 0.05	439	59.9%
		< 1% FDR	344	46.9%

809

810 **Table 6. Empirical quantiles of DeltaCon similarities, ENQUIRE- and STRING-based edges**  
811 **counts, sorted by number of genes in the network.** Median values with respect to each metric and  
812 range of gene counts are highlighted in bold.

Metric	Range of gene counts	Quantiles				
		0%	25%	50%	75%	100%
<b>DeltaCon</b>	4-9	0.75	0.83	<b>0.87</b>	0.94	1.00
	10-14	0.67	0.78	<b>0.81</b>	0.83	1.00
	15-23	0.65	0.74	<b>0.77</b>	0.79	0.87
	24-119	0.56	0.65	<b>0.69</b>	0.72	0.81
<b>Edge count - ENQUIRE</b>	4-9	4	6	<b>7</b>	8	16
	10-14	6	8	<b>10</b>	13	43
	15-23	8	13	<b>17</b>	22	66
	24-119	18	36	<b>49</b>	77	295
<b>Edge count - STRING</b>	4-9	4	6	<b>8</b>	10	23
	10-14	6	11	<b>15</b>	20	50
	15-23	10	21	<b>28</b>	37	94
	24-119	19	54	<b>89</b>	146	591
<b>Connected components - ENQUIRE</b>	4-9	1	2	<b>2</b>	3	5
	10-14	1	3	<b>4</b>	5	8
	15-23	1	4	<b>6</b>	7	12
	24-119	1	4	<b>6</b>	7	15
<b>Connected components - STRING</b>	4-9	1	1	<b>2</b>	2	5
	10-14	1	2	<b>2</b>	3	6
	15-23	1	2	<b>3</b>	4	8
	24-119	1	2	<b>2</b>	4	12

## FIGURES

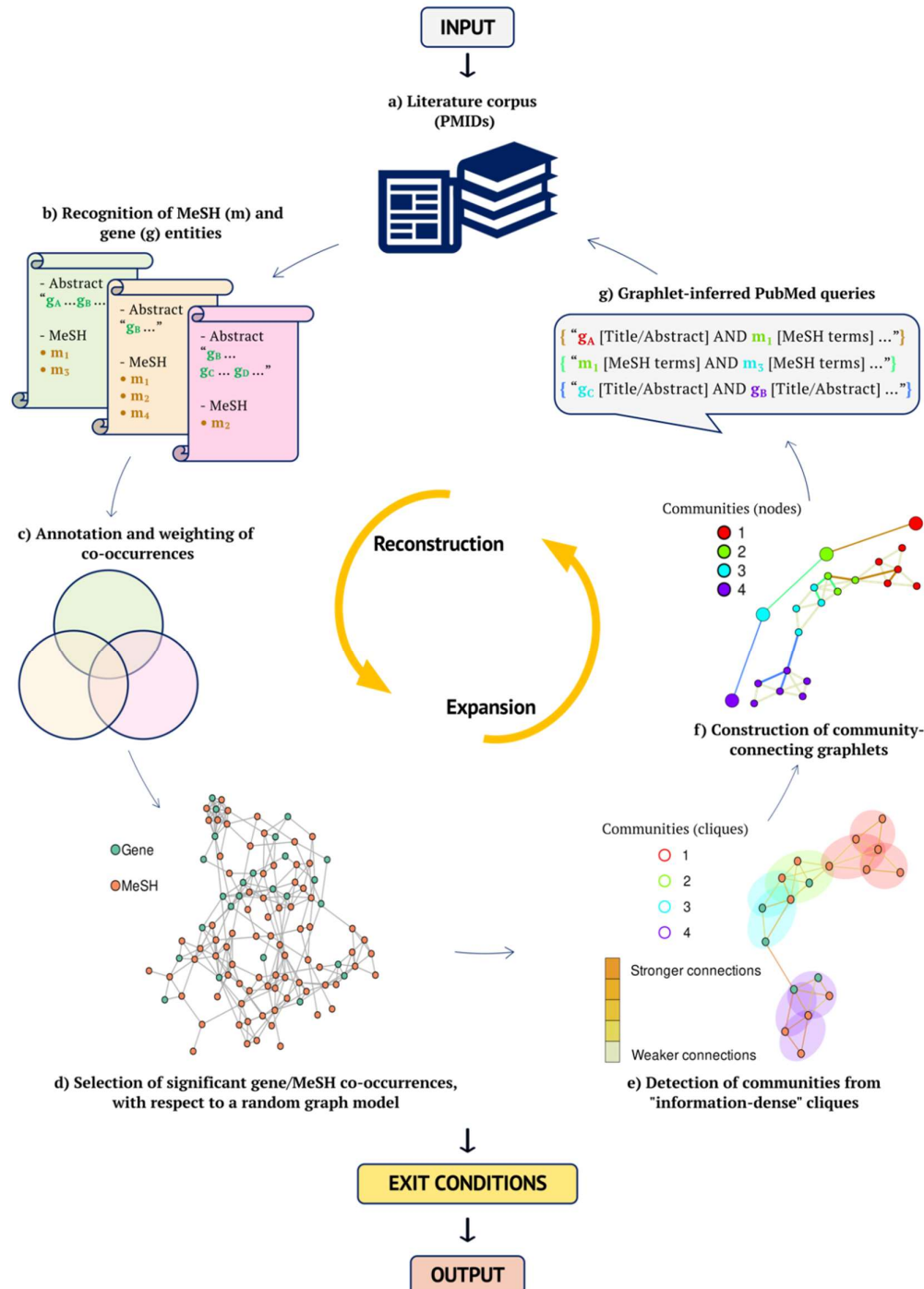


**Fig. 1. Overview of ENQUIRE methodology.** ENQUIRE accepts a set of PubMed identifiers as input, together with optional, user-specified parameters. The pipeline iteratively orchestrates reconstruction and expansion of literature-derived co-occurrence networks, until an exit condition is fulfilled. Additional information about each alphabetically indexed module and output is provided in the **Mat.Met.** section. For a more detailed flowchart, see **Supp. Fig. 1**.

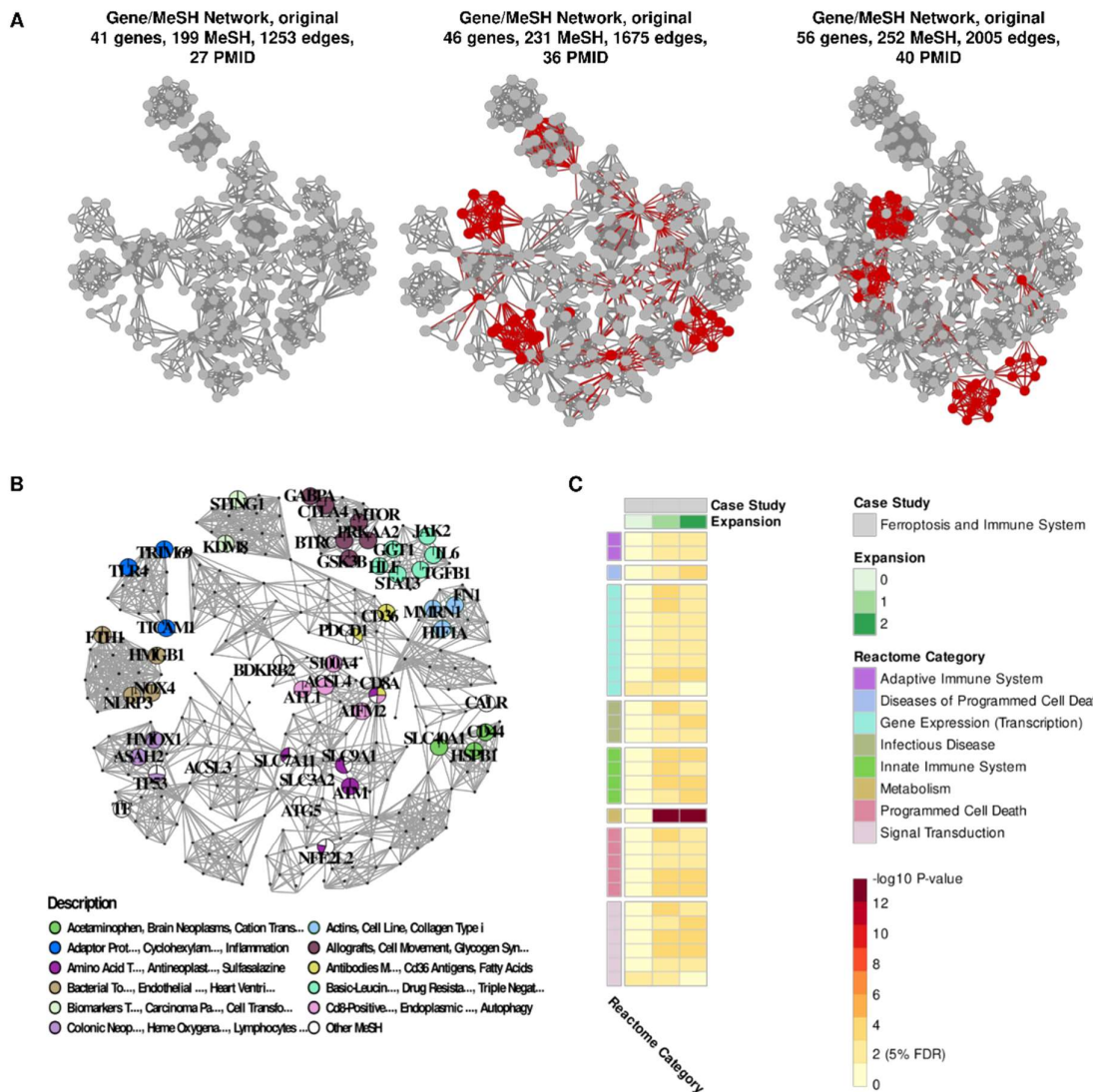


**Fig. 2. Example of ENQUIRE's network reconstruction, expansion and post-hoc analyses.** We used the PubMed identifiers (PMIDs) obtained from the query (“Ferroptosis”[MeSH terms] AND “Immune System”[MeSH terms]) NOT “review”[Publication Type] as input. **A:** visualization of ENQUIRE's network expansion process. Newly found nodes and edges are indicated in red at each expansion. **B:** output of the automatic gene set reconstruction, using the original Gene/MeSH network as input and fuzzy c-means. For simplicity, only nodes referring to genes are enlarged and labelled, and a shortened description of computed gene sets of size 2 or bigger is provided. Sector sizes of the pie-chart-shaped nodes reflect their relative membership degree with respect to each cluster. **C:** topology-based enrichment analysis of Reactome pathways, using original and expanded networks, as described in the Methods section. 30 pathways whose adjusted p-value was significant in at least two networks are depicted. Reactome pathways are grouped based on “Top-Level Pathway” and “Disease” categories. FDR: Holm's family wise error rate.

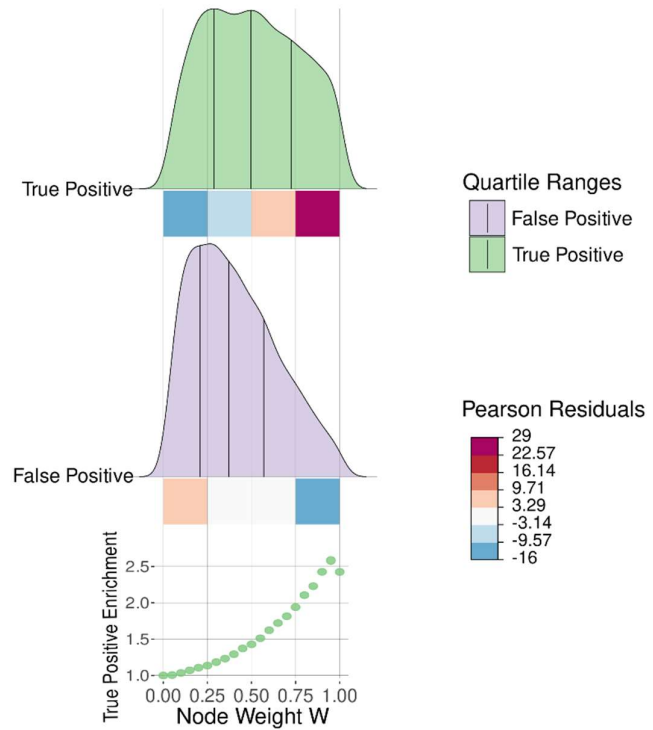


**Fig. 3. Node weight distribution of ENQUIRE-derived gene networks correlate with relevance to the input literature corpus.** We defined true and false positives genes according to their presence or absence in a Reactome pathway, whose reference literature was used to retrieve gene mentions via ENQUIRE's gene normalization and network reconstruction. The statistics shows the aggregated results from 720 Reactome-derived input corpora. The aggregated distributions for true and false positive genes are segmented into quartiles. We defined four ranges of the node score  $W$ , indicated by squares, whose colors reflect Pearson standardized residuals resulting from a significant chi-square statistic. The lower chart depicts the enrichment of true positive genes, after pruning ENQUIRE-derived networks based on different values of  $W$ . Values are relative to the original proportion of true positives.

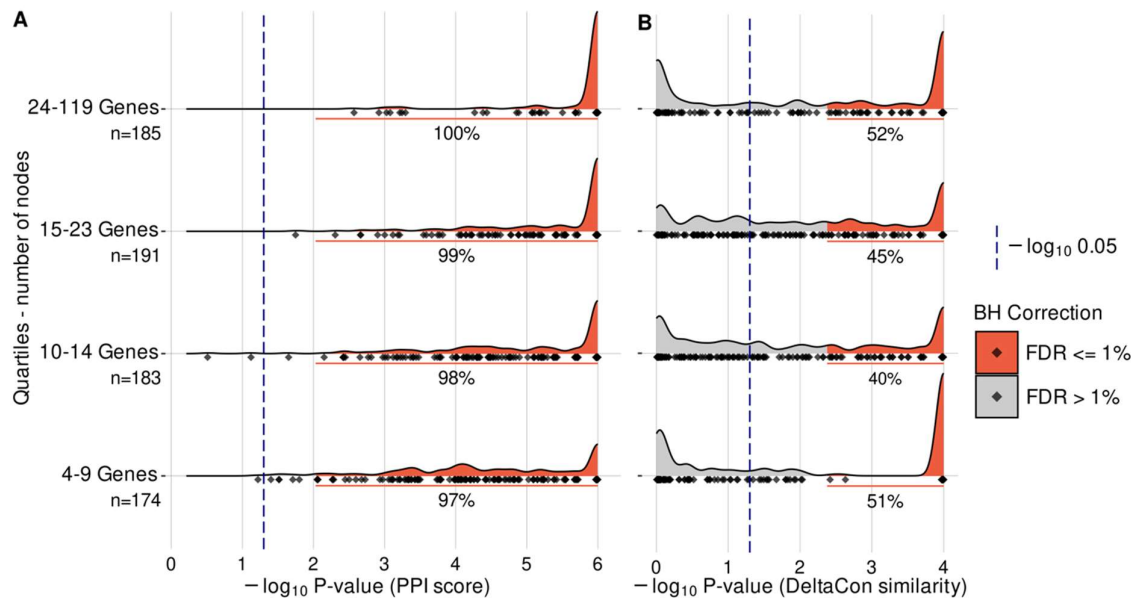


**Fig. 4. Protein-coding genes from ENQUIRE-generated graphs significantly share functional associations.** Panels (A) and (B) respectively report the unadjusted p-value density distributions of STRING-informed edge counts and DeltaCon similarities, arranged by number of protein-coding genes (network size). We used the *H. sapiens* functional association network from STRING to evaluate ENQUIRE-derived networks of protein-coding genes. We tested 733 networks having 10 or more possible network realizations given the observed degree sequence. For each observed network size and degree sequence of ENQUIRE-generated gene networks, 1,000,000 and 10,000 samples were respectively generated to perform a test statistic on the observed edge counts and DeltaCon similarities. See **Mat.Met.** for additional information. The 733 tested networks are apportioned into quartiles based on network size, and for each the exact size is indicated (n). Within each network size interval, grey and red areas respectively highlight insignificant and significant p-values with respect to a globally-applied Benjamini-Hochberg correction (BH), and a percentage is indicated for those below 1% FDR. Diamonds indicate the observed data.

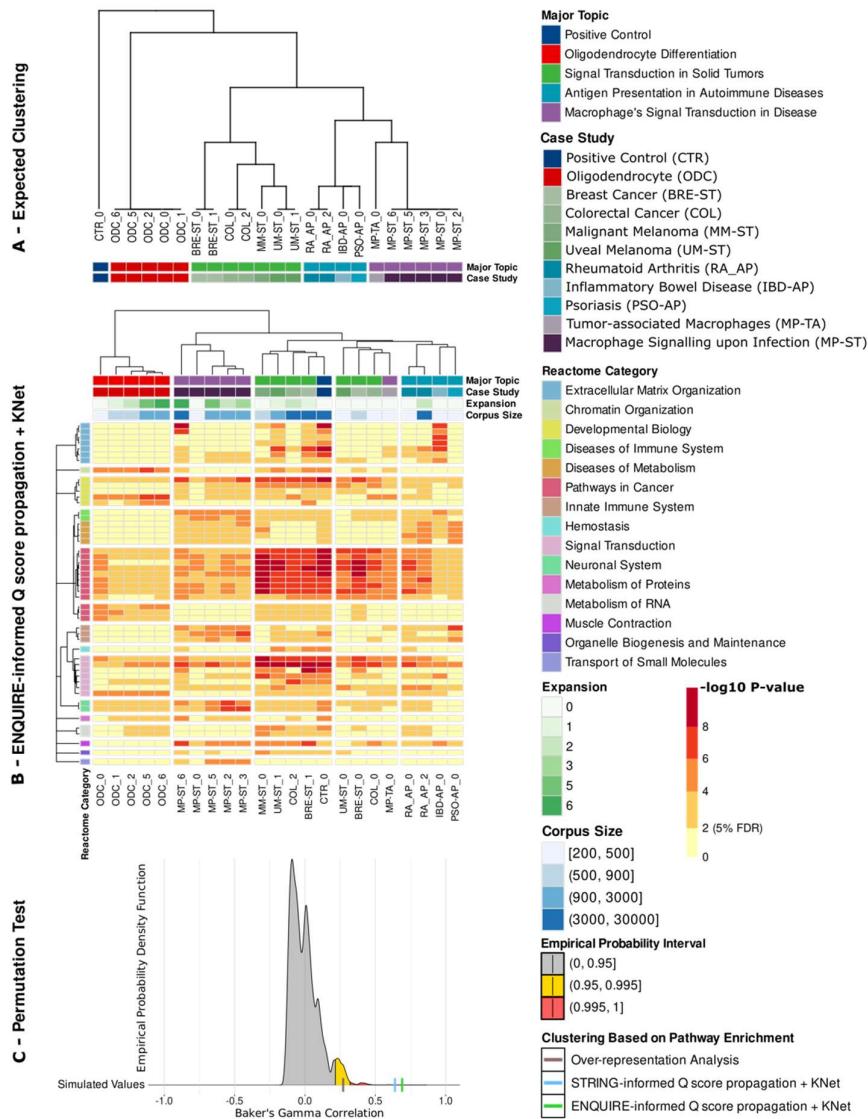
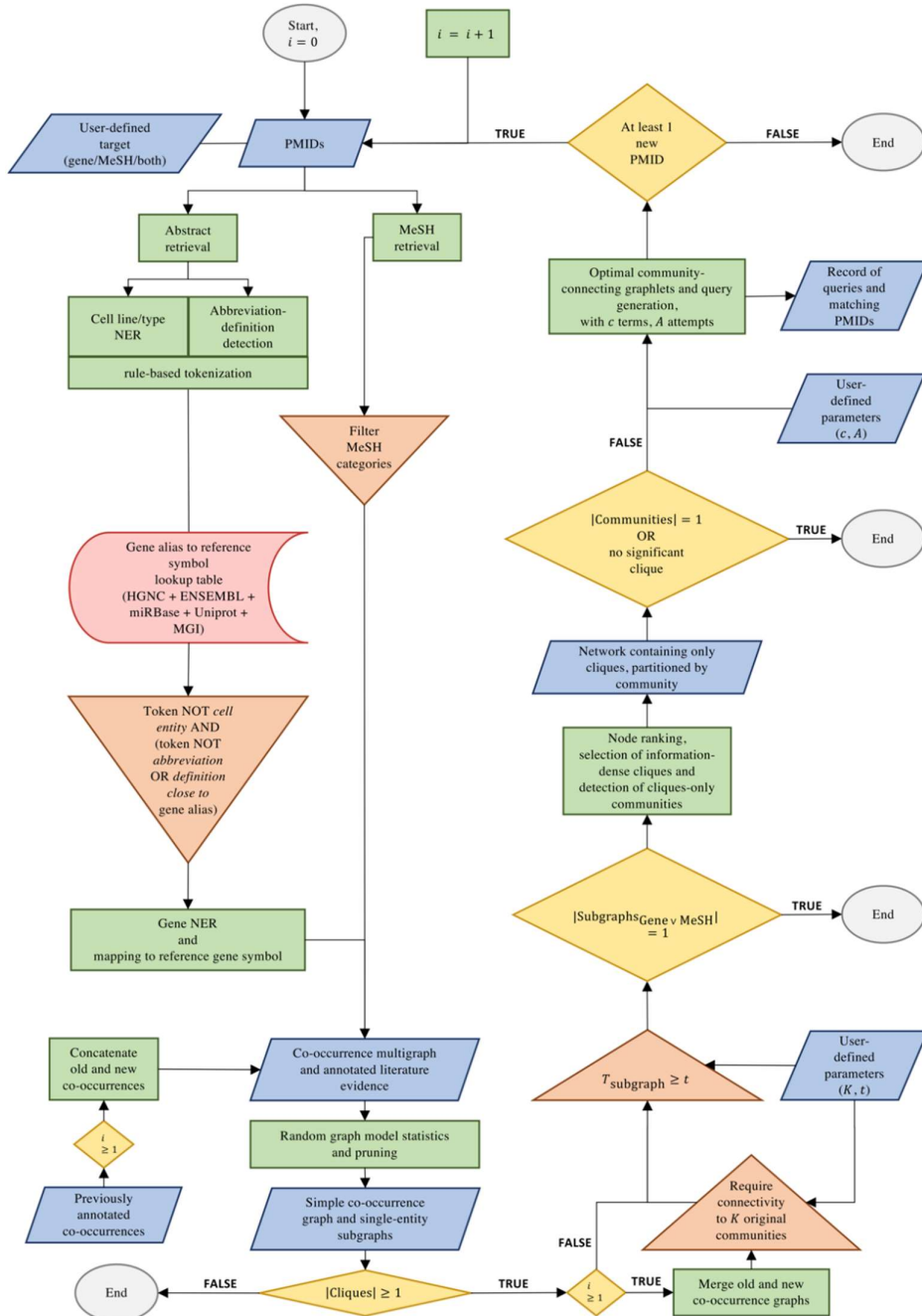
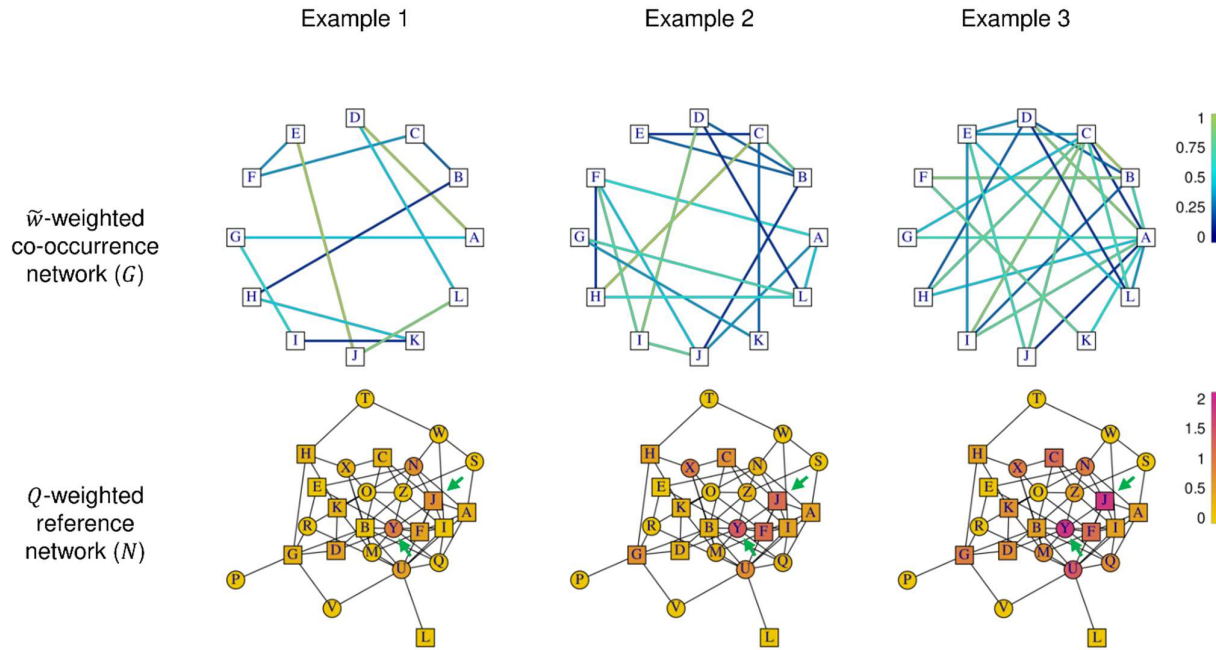


**Fig. 5. ENQUIRE-generated graphs enhance the context resolution of pathway enrichment analyses.** A: reference dendrogram showcasing the expected categorization of the case studies described in **Table 1**. The number following a case study abbreviated name indicates the expansion counter. Network expansions that did not yield any new gene were excluded. B: Topology-based pathway enrichment, obtained by applying *Q* score propagation and SANTA's KNet function on ENQUIRE-informed gene-gene associations (see Post Hoc Analyses under **Mat.Met.**). The heatmap shows the unadjusted p-values for the 50 enriched Reactome pathways with at least one significant, adjusted p-value (5% FDR) and highest variance across case studies (the dendrogram was computed on the complete statistic). Pathways are clustered according to Reactome's internal hierarchy. We respectively apportioned the dendograms into 5 and 15 partitions to visualize their coherence to Major Topic and Reactome Categories. Legends for expansions, rounded corpus size, and p-values ranges are provided. C: Permutation tests of Baker's gamma correlation between the reference dendrogram (A) and clustering obtained from alternative pathway enrichment analyses, as in B. Colored areas indicated probability intervals obtained from simulating correlations between reference and sampled dendograms. See **Mat.Met.** for further details.

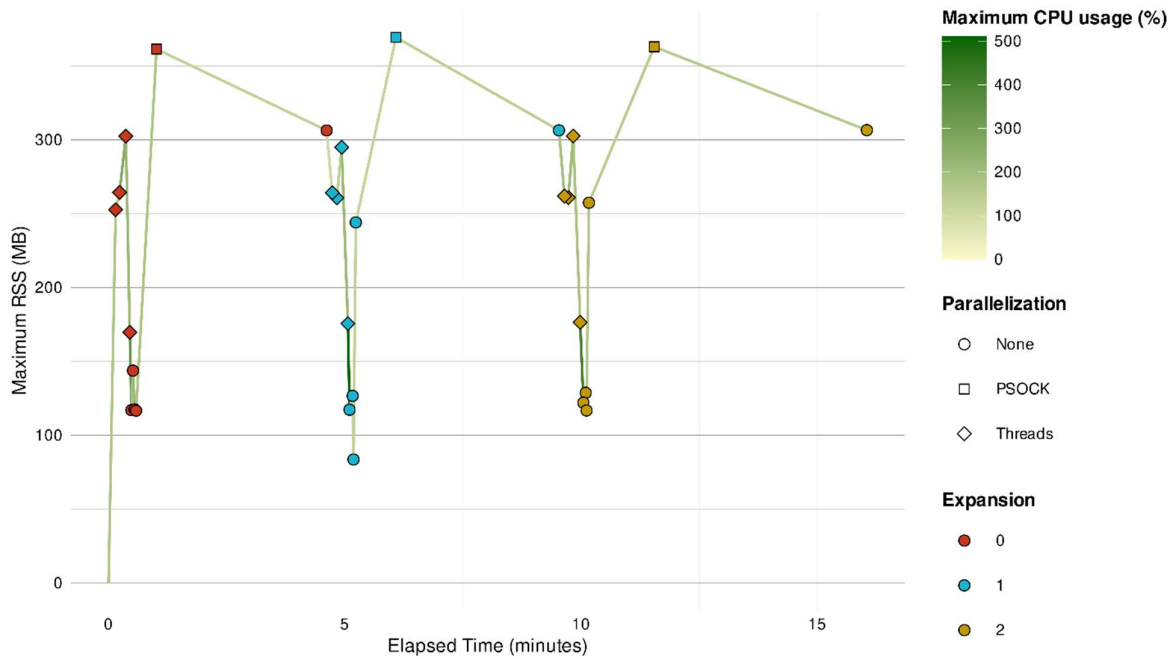
## EXTENDED DATA (SUPPLEMENTARY FIGURES)



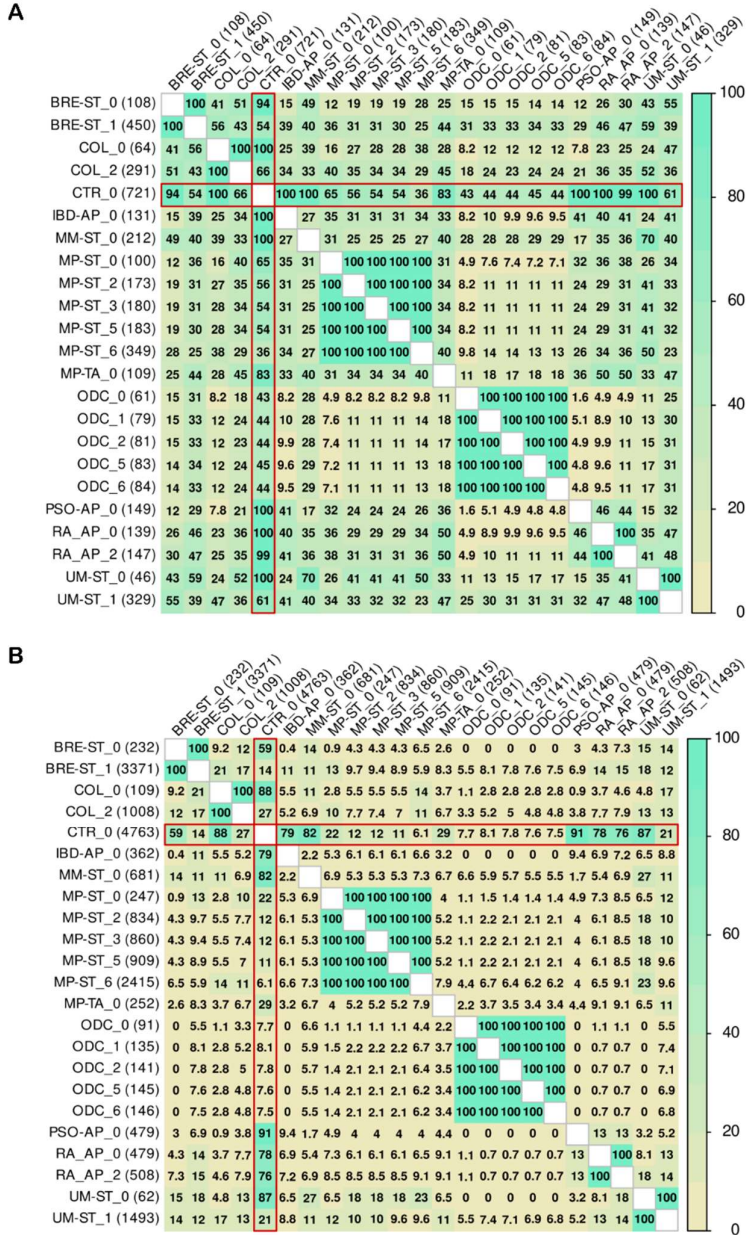
**Supplementary Figure 1. ENQUIRE's flowchart.** The pipeline's schematic is described with respect to start and end points (grey ellipses), input, parameters, and generated data (blue parallelograms), algorithms (green rectangles), filtering (red triangles), pre-computed data (pink halfpipes), and branching points (yellow diamonds). NER: named-entity recognition. PMID: PubMed identifier. MeSH: Medical Subject Heading. Detailed explanation of the parameters and algorithms is provided in the main text.



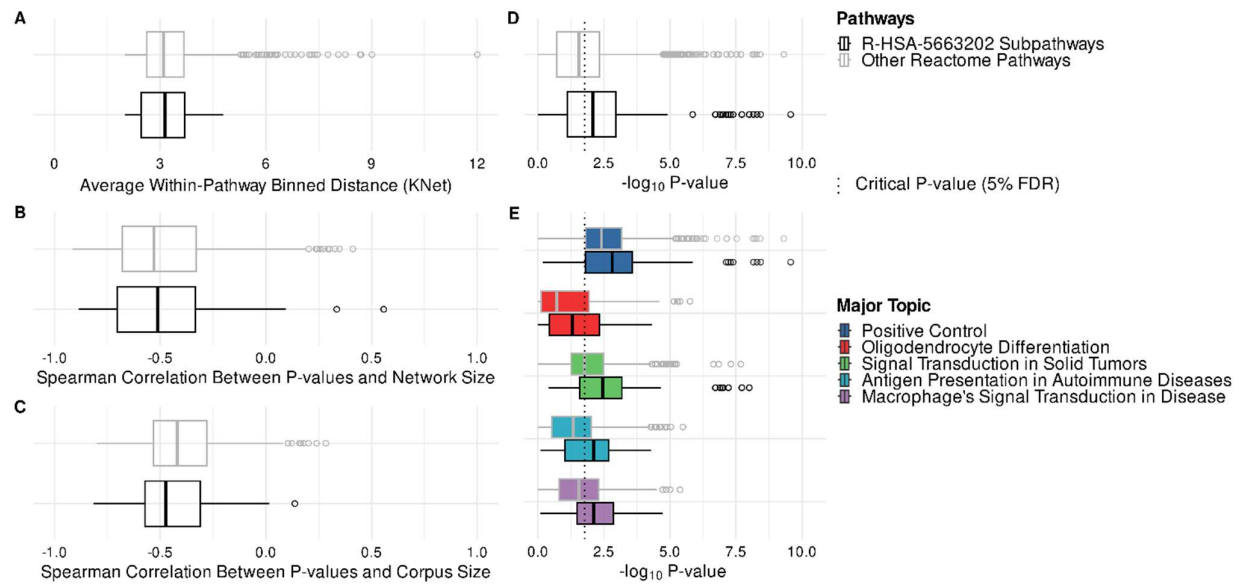
**Supplementary Figure 2. Example of Q score weighting.** The top row shows three simulated co-occurrence networks  $G$  with the same set of textmined genes (squares), generated with progressively higher edge-forming probability, and sampling edge weights  $\tilde{w}$  from a uniform distribution in  $[0,1]$ . Genes from an immutable reference network  $N$  containing both textmined and non-textmined genes (circles) are weighted by the  $Q$  score. For each gene  $g$  in  $N$ , its weight  $Q$  is a function of the textmined genes in the  $g$ -neighbourhood and their  $\tilde{w}$ -weighted distances in the network  $G$ . Nodes with relatively more connections to textmined nodes in the reference network possess higher  $Q$  scores, irrespective of being textmined or having a high node degree. See the non-textmined node Y and the textmined node J as an example.



**Supplementary Figure 3 Memory and CPU usage of a typical ENQUIRE run.** The chart shows the performance monitoring of the exemplary ENQUIRE run described in Results and **Fig. 2**, in which 2 expansions for a total of three iterations were performed. We used a Linux computer with 8 CPUs (2.5 GHz) and 16 GB of RAM. 6 cores were used for parallelization. Each dot represents a submodule launched by ENQUIRE, with the elapsed time at which it terminated as x-coordinate, and the maximum registered RAM usage, in the form of Resident Set Size (RSS, in megabytes), as y-coordinate. Cumulative elapsed time at the end of each reconstruction-expansion cycle is indicated. Lines in-between processes are colored by the maximum CPU usage, which is defined as the used CPU time divided by the time the process has been running, in percentage. This estimate does not typically add up to 100%. Higher CPU usage imply higher workload for each of the utilized cores. Resource usage of parallel socket cluster (PSOCK) protocol can be underestimated, as this protocol generates parallel processes whose process identifiers (PIDs) are independent of ENQUIRE's PID and not monitored. Nevertheless, ENQUIRE restricts the memory usage of PSOCK-based parallel processes, so that their aggregated memory usage is always less than 25% of the available RAM at a given time, possibly reducing the effective number of cores used.



**Supplementary Figure 4. Diversity in nodes and edges from reconstructed and expanded networks generated by ENQUIRE.** We computed similarity measures between ENQUIRE-inferred, co-occurrence gene networks based on the case studies described in **Tsable 1**. The number following a case study abbreviated name indicates the expansion counter. Network expansions that did not yield any new gene were excluded. Panel **A** depicts similarities between the networks' node sets, while panel **B** depicts similarities between edge sets. Numbers and color gradient report Szymbkiewicz-Simpson overlap coefficient percentages (OC). An OC of 0 % indicates no overlap, while an OC of 100% indicates the smaller node or edge set is a subset of the larger one. By construction, same-case-study original and expanded networks possess OCs of 100% with each other. OC between the positive control (CTR) and other case study networks are highlighted in red



**Supplementary Figure 5. Constitutively enriched subpathways of *Diseases of signal transduction by growth factor receptors and second messengers* (R-HSA-5663202).** **A:** differences in network distances between genes belonging to R-HSA-5663202 subpathways and other Reactome pathways, based on STRING's reference physical network (FDR-adjusted p-value = 0.27, Mann-Whitney U test). The binned network distances are used by KNet to compute a topology-based pathway enrichment. **B:** differences in Spearman correlations between KNet p-values and network size, in R-HSA-5663202 subpathways and other Reactome pathways (FDR-adjusted p-value = 0.79, Mann-Whitney U test). **C:** differences in Spearman correlations between KNet p-values and corpus size, in R-HSA-5663202 subpathways and other Reactome pathways (FDR-adjusted p-value = 0.23, Mann-Whitney U test). **D:** differences in p-value distributions between R-HSA-5663202 subpathways and other pathways, across all case studies (FDR-adjusted p-value =  $6.5 \cdot 10^{-5}$ , mixed model ANOVA). **E:** differences in p-value distributions between R-HSA-5663202 subpathways and other pathways, for each major topic (FDR-adjusted p-value (Positive Control) = 0.04 – Mann-Whitney U test, FDR-adjusted p-value (Oligodendrocyte Differentiation) =  $1.3 \cdot 10^{-2}$ , FDR-adjusted p-value (Signal Transduction in Solid Tumors) =  $1.4 \cdot 10^{-4}$ , FDR-adjusted p-value (Antigen Presentation in Autoimmune Diseases) =  $2.3 \cdot 10^{-5}$ , FDR-adjusted p-value (Macrophage's Signal Transduction in Disease) =  $3.9 \cdot 10^{-4}$  – mixed model ANOVA). See **Supp. Information** for details on the test statistics.